Linköping Studies in Science and Technology
Dissertation No. 2331

2D and 3D Halftoning for Appearance Reproduction

Fereshteh Abedini

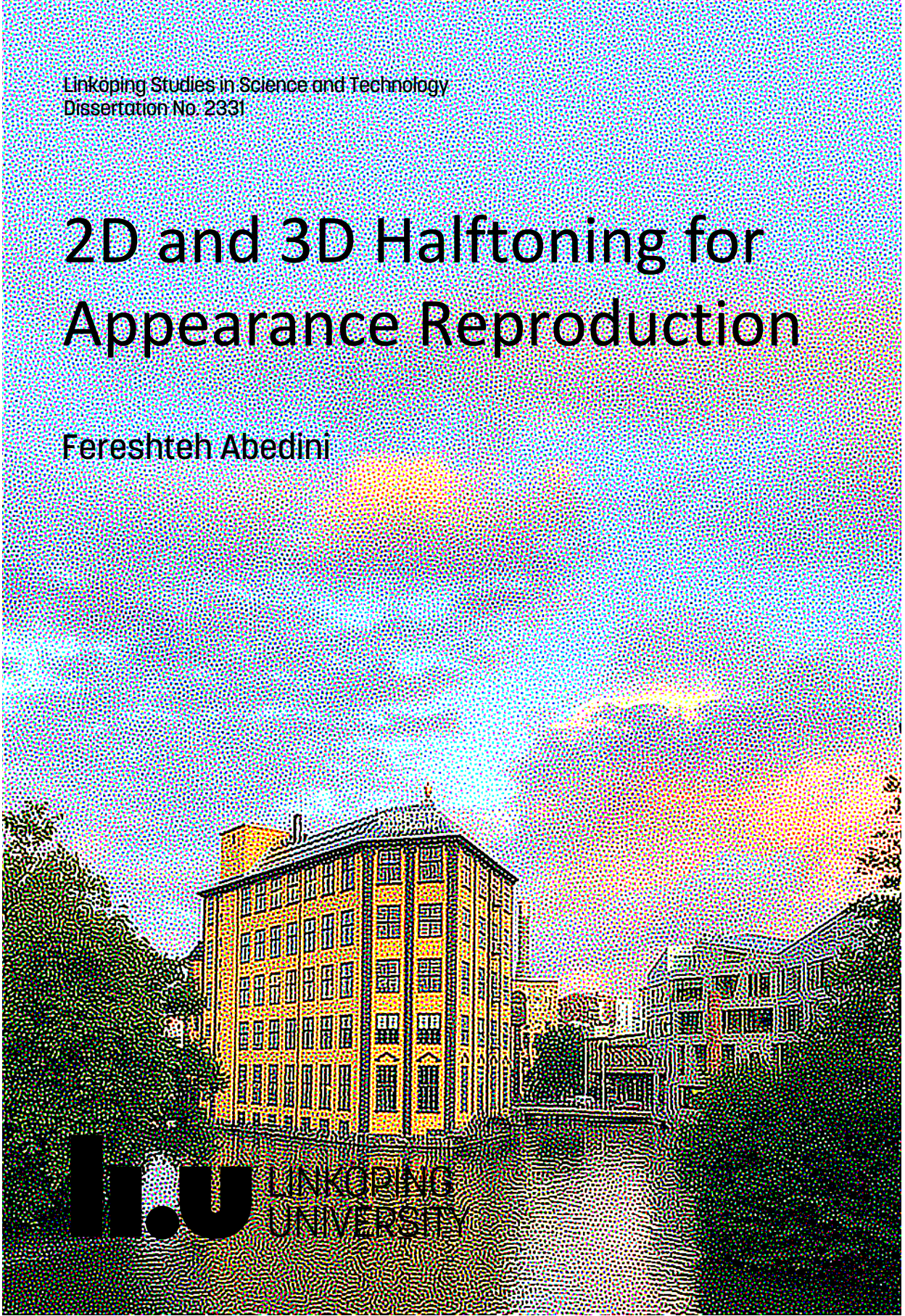

LINKÖPING UNIVERSITY

Linköping Studies in Science and Technology.
Dissertation, No. 2331

2D and 3D Halftoning for Appearance Reproduction

Fereshteh Abedini

Division of Media and Information Technology
Department of Science and Technology
Linköping University, SE-601 74 Norrköping, Sweden
Norrköping, September 2023

Description of the cover image

The cover of this thesis illustrates a second-order FM halftone image generated by the IMCDP halftoning algorithm. The picture shows the Museum of Work (Arbetets museum) located in Norrköping, Sweden. The original image was taken by the author of this thesis.

2D and 3D Halftoning for Appearance Reproduction

Division of Media and Information Technology
Department of Science and Technology
Linköping University, Campus Norrköping
SE-601 74 Norrköping, Sweden

ISBN: 978-91-8075-269-5 (Print)
ISBN: 978-91-8075-270-1 (PDF)

ISSN: 0345-7524

Printed in Sweden by LiU-Tryck, Linköping, 2023

https://doi.org/10.3384/9789180752701

Abstract

The appearance of an object is determined by its chromatic and geometric qualities in its surrounding environment using four optical parameters: color, gloss, translucency, and surface texture. Reconstructing the appearance of objects is of great importance in many applications, including creative industries, packaging, fine-art reproduction, medical simulation, and prosthesis-making. Printers are reproduction devices capable of replicating objects' appearance in 2D and 3D forms. With the introduction of new printing technologies, new inks and materials, and demands for innovative applications, creating accurate reproduction of the desired visual appearance has become challenging. Thus, the appearance reproduction workflow requires improvements and adaptations.

Accurate color reproduction is a critical quality measure in reproducing the desired appearance in any printing process. However, printers are devices with a limited number of inks that can either print a dot or leave it blank at a specific position on a substrate; hence, to reproduce different colors, optimal placement of the available inks is needed. *Halftoning* is a technique that deals with this challenge by generating a spatial distribution of the available inks that creates an illusion of the target color when viewed from a sufficiently large distance. Halftoning is a fundamental part of the color reproduction task in any full-color printing pipeline, and it is an effective technique to increase the potential of printing realistic and complex appearances. Although halftoning has been used in 2D printing for many decades, it still requires improvements in reproducing fine details and structures of images. Moreover, the emergence of new technologies in 3D printing introduces a higher degree of freedom and more parameters to the field of appearance reproduction. Therefore, there is a critical need for extensive studies to revisit existing halftoning algorithms and develop novel approaches to produce high quality prints that match the target appearance faithfully. This thesis aims at developing halftoning algorithms to improve appearance reproduction in 2D and 3D printing.

Contributions of this thesis in the 2D domain is a dynamic sharpness-enhancing halftoning approach, which adaptively varies the local sharpness of the halftone image based on different textures in the original image for realistic appearance printing. The results show improvements in halftone quality in terms of sharpness, preserving structural similarity, and decreasing color reproduction error. The main contribution of this thesis in 3D printing is extending a high quality 2D halftoning algorithm to the 3D domain. The proposed method is

then integrated with a multi-layer printing approach, where ink is deposited at variable depths to improve the reproduction of tones and fine details. Results demonstrate that the proposed method accurately reproduces tones and details of the target appearance. Another contribution of this thesis is studying the effect of halftoning on the perceived appearance of 3D printed surfaces. According to the results, changing the dot placement based on the elevation variation of the underlying geometry can potentially control the perception of the 3D printed appearance. It implies that the choice of halftone may prove helpful in eliminating unwanted artifacts, enhancing the object's geometric features, and producing a more accurate 3D appearance. The proposed methods in this thesis have been evaluated using different printing techniques.

Populärvetenskaplig Sammanfattning

Traditionellt har färgåtergivning i tryck åstadkommits genom att de fyra tryckfärgerna cyan, magenta, gult och svart trycks på ett reflekterande substrat. Att åstadkomma korrekt färgåtergivning kräver modeller för hur bläck, ljus och papper interagerar, för att kunna bestämma optimal placering av tryckfärgerna. För att skapa rätt proportioner av tryckfärgerna används *rastrering*, en process som delar upp tryckfärgerna i rasterpunkter, som varierar i storlek, form eller frekvens. På normalt betraktningsavstånd är de tryckta rasterpunkterna knappt synliga, och man kan med traditionellt "fyrfärgstryck" reproducera ett stort antal kulörer. Rastreringen har stor inverkan på den resulterande bildkvaliteten hos trycket, och påverkar faktorer som skärpa, färgåtergivning, detaljåtergivning, mjuka övergångar och avsaknad av oönskade artefakter.

Med den snabba utvecklingen av nya tryckteknik möjliggörs nu reproduktion även i 2.5D (ofta kallad relieftryck) och i 3D, genom att material med olika optiska egenskaper mixas i tryckprocessen. Där man i konventionellt tryck som bäst kunnat reproducera en tvådimensionell avbild med korrekt färgåtergivning, öppnas nu möjligheten att reproducera det kompletta utseendet av ett objekt eller en yta. Förutom geometriska egenskaper kräver detta kontroll av optiska parametrar som färg, glans, ytstruktur och opacitet. Att reproducera det korrekta utseendet på objekt och ytor är av betydelse i flera tillämpningar, exempelvis förpackningar, reproduktion av konstverk och för naturtrogna medicinska proteser. Utmaningen att naturtroget reproducera inte bara korrekt kulör, utan även naturtrogen ytstruktur, glans och nivå av genomskinlighet, är ett nytt och snabbt växande forskningsområde som ofta refereras till som *appearance printing*.

Även om rastreringsmetoder för konventionellt tryck har vidareutvecklats och förbättrats under flera decennier, finns fortfarande förbättringspotential för högkvalitativ reproduktion av fina detaljer och strukturer. Dessutom introducerar ny skrivteknik en rad problem och utmaningar som först måste lösas, för att till fullo kunna utnyttja potentialen att reproducera naturtrogna ytor och objekt, i fler än två dimensioner. Därför finns det ett behov att vidareutveckla befintliga rastreringsmetoder, samt att utveckla nya, för att kunna reproducera högkvalitativt tryck som matchar inte bara originalets färg, utan alla de optiska parametrar som samverkar i vår upplevelse av en ytas eller ett objekts utseende.

Denna avhandling adresserar flera av de tekniska utmaningarna för att till fullo kunna utnyttja potentialen hos *appearance printing*, genom att utveckla rastre-

ringsmetoder för högkvalitativ reproduktion både i två och tre dimensioner. En nyutvecklad rastreringsmetod för 2D-tryck varierar den lokala skärpan adaptivt beroende på strukturen hos originalbilden, vilket ger en mycket naturtrogen reproduktion av ytstruktur. Vidare har en högkvalitativ rastreringsmetod för 2D-tryck vidareutvecklats för att hantera tryck i tre dimensioner, där reproduktionen av kulörer och fina detaljer sker mycket exakt, genom att tryckfärgernas placering i djupled optimeras. Ytterligare ett bidrag är experiment som påvisar att upplevelsen av struktur och form kan påverkas genom att kontrollera rasterpunkternas form och riktning utifrån höjdinformation i den underliggande geometrin. Sammantaget medför de introducerade metoderna och experimenten både en ökad förståelse för hur rastreringen påverkar olika kvalitetsaspekter, lösningar på praktiska implementationsutmaningar, och ökade möjligheter att till fullo utnyttja potentialen hos moderna tryckteknikers, för ett högkvalitativt tryckresultat.

"Great things are not done by impulse, but by a series of small things brought together, and great things are not something accidental, but must certainly be willed."

Vincent Van Gogh

Acknowledgments

First, and for most, I would like to thank my supervisors, Sasan Gooran and Daniel Nyström, for their unwavering guidance, invaluable insights, and continuous support throughout my PhD studies. Their expertise and commitment have been invaluable in shaping the direction and quality of this research.

I am grateful to have been a part of the ApPEARS project (Appearance Printing European Advanced Research School). This opportunity has afforded me the privilege of learning from many scientists. Special thanks go to Vlado Kitanovski and Aditya Suneel Sole for their valuable contributions to this research.

I want to extend my gratitude to Jonas Löwgren for his willingness to lend a listening ear and his ability to offer constructive solutions. I express my appreciation to our wonderful administrators, Gun-Britt and Agne, whose behind-the-scenes efforts and help were an integral part of this journey.

I am grateful to my friends at the office, Ahmet, Danhua, Yifan, Nithesh, and Tanaboon, for making my PhD life enjoyable. My warmest thanks go to my amazing friends in Norrköping, Behnaz, Elmira, Pouria, Saghi, Ehsan, Mina, Asma, and Amin. Their presence, positive mindset, and kind heart have been treasures throughout this journey. I would also like to thank my friends in Tehran, Sally and Sara, for their encouragement and love despite the distance.

I am deeply grateful to my beloved parents, whose love, sacrifices, dedication, and optimism have always been my pillars of strength, encouraging me to be persistent and hopeful. I thank my lovely sister, Farzaneh, whose determination and ambition have always strengthened and motivated me.

Last but not least, my heartfelt thanks go to Soheil, whose unconditional love and support have been my driving force. His patient listening, insightful discussions, encouragement, and constant reassurance have been my anchor, enabling me to navigate the challenges during my PhD studies.

This journey owes its realization to the invaluable collective support of these remarkable individuals. I am profoundly grateful for their presence in my life and impact on this academic achievement.

Fereshteh
Norrköping, September 2023

List of Publications

This thesis includes research that is based on the following publications:

Paper A

F. Abedini, S. Gooran, and D. Nyström, "3D halftoning based on iterative method controlling dot placement," NIP and Digital Fabrication Conference, vol. 2020, no. 1. Society for Imaging Science and Technology, pp. 69–74, 2020.

Paper B

S. Gooran and F. Abedini, "3D surface structures and 3D halftoning," NIP and Digital Fabrication Conference, vol. 2020, no. 1. Society for Imaging Science and Technology, pp. 75–80, 2020.

Paper C

F. Abedini, S. Gooran, and D. Nyström, "The effect of halftoning on the appearance of 3D printed surfaces," The Advances in Printing and Media Technology: Proceedings of the 47th International Research Conference of IARIGAI, pp. 237–243, 2021.

Paper D

F. Abedini, S. Gooran, V. Kitanovski, and D. Nyström, "Structure-aware halftoning using the iterative method controlling the dot placement," Journal of Imaging Science and Technology, pp. 060404-1 - 060404-14, 2021.

Paper E

F. Abedini and S. Gooran, "Structure-aware color halftoning with adaptive sharpness control," Journal of Imaging Science and Technology, pp. 060404-1 - 060404-11, 2022.

Paper F

F. Abedini, A. Trujillo-Vazquez, S. Gooran, and S. Klein, "Effect of halftones on printing iridescent colors," Electronic Imaging, pp. 206-1 - 206-6, 2023.

Paper G

F. Abedini, R. Hlayhel, S. Gooran, D. Nyström, and A. Suneel Sole, "Multi-layer halftoning for poly-jet 3D printing," London Imaging Meeting. Society for Imaging Science and Technology, 2023.

Other publications by the author that are relevant to this thesis but are not included:

- R. Tonello, F. Abedini, D. B. Pedersen, and J. Revall, "Fast impression painting using multi-color fused deposition modeling with a diamond hotend," in 2022 Summer Topical Meeting: Advancing Precision in Additive Manufacturing, 2022.
- S. Gooran and F. Abedini, "Three-dimensional adaptive digital halftoning," Journal of Imaging Science and Technology, pp. 060 403–1 – 060 403–12, 2022.
- A. Trujillo-Vazquez, F. Abedini, A. Pranovich, C. Parraman, S. Klein, "Prints with *tonalli*: Reproducing featherwork from pre-colonial Mexico using structural colorants," Submitted to Journal of Colorants, MDPI, July 2023.

Summary of Contributions

This thesis is focused on *Halftoning for Appearance Printing*. Halftoning is essential both in 2D and 3D printing. 3D halftoning has been studied and addressed in papers *A*, *B*, *C*, and *G*. Papers *D*, *E*, and *F* have focused on improving 2D halftoning. Publications included in this thesis with a brief description and contributions of the author of this thesis are listed below.

Paper A: 3D halftoning based on iterative method controlling dot placement

F. Abedini, S. Gooran, and D. Nyström, "3D halftoning based on iterative method controlling dot placement," NIP and Digital Fabrication Conference, vol. 2020, no. 1. Society for Imaging Science and Technology, pp. 69–74, 2020. Full paper can be downloaded using this link.

This paper focuses on improving appearance reproduction in 3D printing by developing a 3D iterative halftoning method. The article studies the aspects of adapting and applying the Iterative Method Controlling Dot Placement (IMCDP) to halftone three-dimensional surfaces. The main goal is to extend the 2D algorithm to a 3D halftoning approach with minor modifications. The result was published as a conference paper at the Printing for Fabrication Conference 2020. It was presented remotely at that conference by the author of this thesis (Virtual event due to the Covid-19 pandemic).

The author contributed to developing the idea, implementing it, and writing the complete first draft of the manuscript.

Paper B: 3D surface structures and 3D halftoning

S. Gooran and F. Abedini, "3D surface structures and 3D halftoning," NIP and Digital Fabrication Conference, vol. 2020, no. 1. Society for Imaging Science and Technology, pp. 75–80, 2020. Full paper can be downloaded using this link.

In this paper, the developed 3D IMCDP in *Paper A* is used to apply different halftone structures on 3D surfaces to investigate the potential improvement/control of the appearance reproduction of 3D surfaces through halftoning. It focuses on using different halftones based on the 3D geometrical structure of the surface and/or the viewing angle in combination with the structure of the texture being mapped on the surface. The result was published as a conference paper at the Printing for Fabrication Conference 2020.

The author was part of the implementation and assisted in writing.

Paper C: The effect of halftoning on the appearance of 3D printed surfaces

F. Abedini, S. Gooran, and D. Nyström, "The effect of halftoning on the appearance of 3D printed surfaces," The Advances in Printing and Media Technology: Proceedings of the 47th International Research Conference of IARIGAI, pp. 237–243, 2021. Full paper can be downloaded using this link.

This work uses the methods and simulations results in *Paper A* and *Paper B* to practically evaluate the findings in these two papers through printing them using a commercial 3D printer. The result was published as a conference paper at the IARIGAI conference in 2021 and was presented remotely by the author of this thesis (Hybrid event due to the Covid-19 pandemic).

The author was the main contributor to the implementing, printing samples, and writing the first complete draft of the manuscript.

Paper D: Structure-aware halftoning using the iterative method controlling the dot placement

F. Abedini, S. Gooran, V. Kitanovski, and D. Nyström, "Structure-aware halftoning using the iterative method controlling the dot placement," Journal of Imaging Science and Technology, pp. 060404-1 - 060404-14, 2021. Full paper can be downloaded using this link.

This paper contributes to the improvement of 2D appearance reproduction. The paper proposes a structure-aware alternative to the IMCDP halftoning algorithm to improve the halftone image quality in terms of sharpness, structural similarity, and tone preservation. The result was published in the Journal of Imaging Science and Technology 2021. It was also presented remotely at the Electronic Imaging conference in January 2022 by the author of this thesis (Virtual event due to the Covid-19 pandemic).

The author contributed to developing the idea, implementing, analyzing results, and writing the complete first draft of the manuscript.

Paper E: Structure-aware color halftoning with adaptive sharpness control

F. Abedini and S. Gooran, "Structure-aware color halftoning with adaptive sharpness control," Journal of Imaging Science and Technology, pp. 060404-1 - 060404-11, 2022. Full paper can be downloaded using this link.

This paper contributes to the improvement of 2D appearance reproduction. The proposed method in *Paper D* is a monochrome halftoning technique, the degree of sharpness enhancement is constant for the entire image, and the algorithm is prohibitively expensive for large images. In *Paper E*, a faster and more flexible approach for extracting the image structure is presented. The method adaptively varies the local sharpness of the halftone image based on different textures across the original image, and it is also extended to color halftoning. The result was published in the Journal of Imaging Science and Technology 2022 and presented at the Electronic Imaging conference in January 2023.

The author was the main contributor in developing the idea, implementing, analyzing results, and writing the complete first draft of the manuscript.

Paper F: Effect of halftones on printing iridescent colors

F. Abedini, A. Trujillo-Vazquez, S. Gooran, and S. Klein, "Effect of halftones on printing iridescent colors," Electronic Imaging, pp. 206-1 - 206-6, 2023. Full paper can be downloaded using this link.

This paper contributes to improving the 2D appearance reproduction of iridescent colors. In this work, the performance of the structure-aware color halftoning proposed in *Paper E* is evaluated using RGB pigments inks via a custom printer (screen printing). The project is a case study to find suitable ways to reproduce and present the visual appearance of an original object, including its three-dimensional features, through printing. The result was published as a conference paper in the Electronic Imaging Conference 2023.

The author mainly contributed to implementing, creating, and adapting halftones for handmade screen printing. She also wrote the majority of the first draft of the manuscript.

Paper G: Multi-layer halftoning for poly-jet 3D printing

F. Abedini, R. Hlayhel, S. Gooran, D. Nyström, and A. Suneel Sole, "Multi-layer halftoning for poly-jet 3D printing," London Imaging Meeting. Society for Imaging Science and Technology, 2023.

In this paper, the 3D halftoning algorithm, developed in *Paper A*, is integrated with a multi-layer printing approach, where ink is deposited at variable depths to improve the reproduction of tones and fine details. The method was evaluated using the voxel printing utility of a poly-jet 3D printer. According to the results, the proposed method accurately reproduces tones and details of the target appearance. The paper is published in the proceedings of the London Imaging

Meeting 2023.

The author developed and implemented the method and converted the output to a readable format for the printer. She took part in analyzing the results and wrote the majority of the first draft of the manuscript.

Contents

Abstract v

Populärvetenskaplig Sammanfattning vii

Acknowledgments xi

List of Publications xiii

Summary of Contributions xv

1 Introduction 1
- 1.1 Visual Appearance 1
- 1.2 Appearance Reproduction 3
- 1.3 Halftoning for Appearance Reproduction 4
- 1.4 Thesis Objectives 7
- 1.5 Thesis Outline 8

2 Fundamentals of Digital Halftoning 9
- 2.1 Halftone Structure 9
- 2.2 Halftoning Algorithms 12
  - 2.2.1 Threshold Halftoning 12
  - 2.2.2 Error Diffusion Halftoning 15
  - 2.2.3 Iterative Halftoning 15
- 2.3 Color Halftoning 20
- 2.4 Structure-Aware Halftoning 21
- 2.5 Quality Evaluation of Halftone Images 24
  - 2.5.1 Mean Squared Error 26
  - 2.5.2 Spatial CIELAB 26
  - 2.5.3 Structural Similarity Index Measure 27
  - 2.5.4 Blur Factor 28
- 2.6 3D Printing and 3D Halftoning 29
  - 2.6.1 Voxelization 30
  - 2.6.2 Layer Construction 32
  - 2.6.3 Color Management 32
  - 2.6.4 Material Arrangement 32

3 Main Contributions of the Thesis 35
- 3.1 Extending 2D IMCDP to 3D Halftoning 35

3.2 Developing a Structure-Aware IMCDP 38
3.3 Effect of Halftoning on Appearance of 3D Prints 40
3.4 Challenges in Adapting Halftones to New Inks in 2D Prints 42

4 Concluding Remarks and Future Work 45
4.1 Concluding Remarks 45
4.2 Insights into the Future Work 47

Bibliography 49

Appendix - Publications 59

CHAPTER 1

Introduction

1.1 Visual Appearance

The concept of visual appearance encompasses many factors that contribute to the overall perception of an object within the surrounding environment in which it is observed. Visual appearance involves the interplay of color, shape, surface texture, gloss, transparency, and opacity, as well as how all these parameters interact to deliver a perception. According to the visual appearance measurement framework of CIE (Commission Internationale de l'Eclairage – International Commission on Illumination), appearance may be defined as:

> *"Appearance is the visual sensation through which an object is perceived to have attributes such as size, shape, color, texture, gloss, transparency, opacity, etc." [1]*

Visual appearance is pivotal in shaping perceptions and influencing judgments and choices. Therefore, the measurement and quantification of its properties are highly demanded in almost all manufacturing industries. The entanglement of diverse factors makes it very complicated to scale the visual appearance through only one physical metric; therefore, its characterization is described through four principal optical parameters of materials: color, gloss, translucency, and

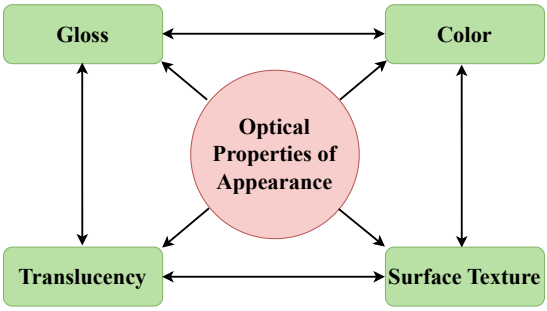

Figure 1.1 — *Sub-division of optical properties of appearance and their mutual interactions [1].*

surface texture [1, 2]. Figure 1.1 shows these groups and their interactions.

Color refers to the visual sensation resulting from the interaction between the light source (the illuminant), the object (usually a reflecting surface), and the human visual system (the detector) [1, 3]. With normal color perception, the human visual system has three types of retinal cells, known as cones, equipped with photosensitive pigments sensitive to distinct wavelengths of light. These three cones (called S, M, and L) represent the visible electromagnetic spectrum's short, medium, and long wavelength regions, respectively. A beam of light that contains mostly short wavelengths of the visible light spectrum stimulates the S cone, and that light is perceived as the color blue. Similarly, when a beam of light primarily consists of medium wavelengths from the visible light spectrum, it activates the M cone, resulting in the perception of the color green, and a beam of light that contains mostly long wavelengths of the visible light spectrum triggers the L cones, leading to the perception of the color red. Rays of light having different wavelengths stimulate signals from the three cones mixed in different proportions, enabling the human visual system to perceive a broad range of colors [3].

Gloss refers to the perceptual quality of a surface associated with how it reflects light and its ability to exhibit light reflection near the specular direction [4]. Gloss arises from the interaction between light and microstructures of a surface. Microstructures influence the direction and intensity of light reflection. Smooth surfaces, which reflect light in a well-defined manner, are characterized as glossy, while rough or textured surfaces have lower gloss due to light scattering in multiple directions. The definition of the perception of gloss, as well as its

characterization and quantization, remain open study objectives [1].

Translucency is an intermediate state between complete transparency and complete opacity, where some light is transmitted but not to the extent of absolute clarity, some light is reflected, and some is scattered [1, 4]. Translucency arises due to the interaction of light with the microstructure and composition of the component materials and characterizes subsurface light transport through objects and materials [5].

Surface texture refers to the physical attributes and characteristics of a surface associated either with physical and topological variability in a surface or spatial variation in appearance caused by the nonuniformity of materials within the object (sub-surface texture). Surface texture is generally described using terms like fine, coarse, grained, rough, and smooth [1].

1.2 Appearance Reproduction

Appearance reproduction refers to the capability of reproducing the visual characteristics and aesthetics of an object or surface. It involves reproducing the color, gloss, translucency, surface texture, and other visual attributes with high fidelity. Appearance reproduction finds applications in diverse fields, including design, art, fashion, manufacturing, architecture, packaging, medical simulation, prosthesis making, and entertainment industries. Accurate reproduction of the "look" and "feel" of the object is critical in all of these applications. It has been shown that the four appearance attributes (color, gloss, translucency, and surface texture) are not necessarily independent, and one attribute might be involved in the perception of the others [1]. However, among the four appearance attributes, color reproduction is often sufficient for a high-fidelity appearance reproduction. As such, accurate color reproduction is a critical quality measure in reproducing the desired appearance.

Printers are reproduction devices capable of replicating the appearance of objects with various technologies such as 2D, 2.5D, and 3D printing. Two-dimensional digital printing, commonly associated with traditional inkjet or laser printers, reproduces the visual appearance on flat surfaces, such as photographs, paintings, or graphic designs. Two-and-half dimensional printing, also known as relief printing or elevated printing, goes beyond traditional 2D printing by incorporating relief effects and surface textures. This technique can reproduce the appearance of surfaces with varying heights, resulting in prints that simulate textured materials' visual and tactile qualities. Three-dimensional printing enables the fabrication of 3D physical objects with complex geometries. Advanced

3D printing technologies, such as multi-material or multi-color printing, enable faithful appearance reproduction preserving intricate details, colors, textures, and geometries.

However, printers are devices with a limited number of inks that can either print a dot or leave it blank at a specific position on a substrate. For instance, many 2D printers only use four primary colors: cyan, magenta, yellow, and black, with which a wide range of colors and shades can be reproduced. To create different colors using only a limited number of inks (colorants), an optimal placement of the available inks is needed. *Halftoning* is a technique that deals with this challenge by generating a spatial distribution of the available inks that creates a visual illusion of the target color when viewed from a sufficiently large distance [6, 7]. Halftoning is a fundamental part of color reproduction in full-color printing pipelines and facilitates the simulation of a much wider range of tones and colors than would otherwise be possible.

1.3 Halftoning for Appearance Reproduction

Digital halftoning converts a continuous-tone color image into a set of discrete ink placement binary maps, one for each ink, for printing purposes [6, 7]. An ink placement binary map is a binary image, called a halftone image, consisting of "1"s and "0"s, where "1" at a pixel represents a printed dot at that particular position and a "0" means that the corresponding position should remain blank. Figure 1.2 shows the printing process of a digital color image using the four primary inks cyan (C), magenta (M), yellow (Y), and black (K). The color image, usually in RGB color space, is first converted to CMYK colorant channels. After the separation of color channels, each color channel is halftoned separately, and the final color halftone image is created by superpositioning all color channels [3].

Halftoning methods aim to optimally place the dots to create a visual illusion of the original image. The key idea of halftoning algorithms is based on the fact that the human visual system (HVS) functions as a low-pass filter and attenuates high frequencies. The goal is to minimize the difference (error) between the original continuous-tone image and the halftone image so that the error is shifted to higher frequencies, hardly perceptible by the eyes [6, 7].

Halftoning creates the illusion of different shades of color by varying the size and spacing of the dots. Different variants of halftoning techniques have been proposed for different purposes and printing techniques. For example, as shown in Figure 1.3 (top), larger clusters of closely spaced dots will appear darker than

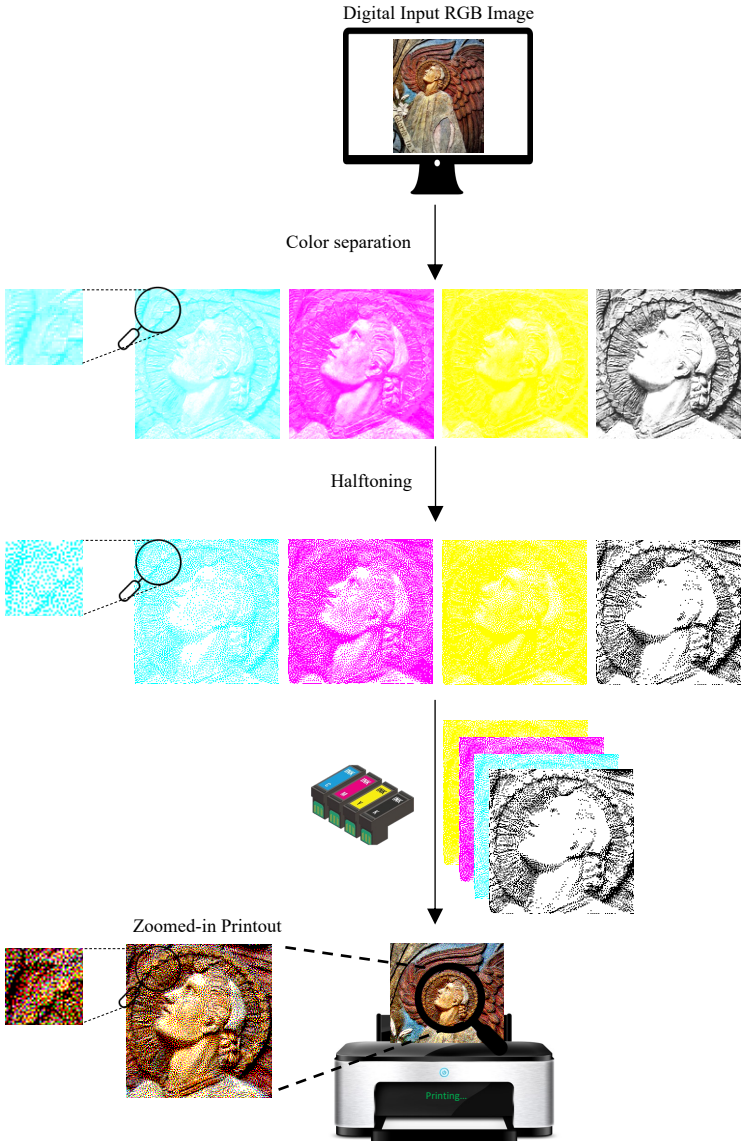

Figure 1.2 — *Diagram of halftoning technique in the printing process of an RGB color digital image using four primary print colorants: cyan, magenta, yellow, and black. For better illustration, color separations, and halftones are shown for an enlarged cropped area of the original image. Because the printer's characteristics were unknown to us, the color halftone images are not adapted to the printer that prints this thesis. As a result, in the printed version of the thesis, the color halftones may not appear in accurate colors.*

smaller clusters of more widely spaced dots. Halftone dots could be dispersed in the form of many single dots of the same size, where the more closely distributed dots corresponds to darker gray levels and the more scattered distributed dots to brighter gray levels. However, printers using electrophotographic technology cannot stably print isolated dots; hence clustered-dot halftones are more suitable for these printers, where the size of the clusters is proportional to the represented gray tone; larger clusters correspond to darker gray tones [8, 9]. Figure 1.3 (bottom) illustrates halftone structures in the form of isolated distributed dots and clustered dots for patches of the same gray tone. (In the printed version of this thesis, they might not appear to be of the same gray tone).

Although halftoning has been used in 2D printing for a long time, accurate reproduction of fine details and structures of images remains a challenge. One of the main shortcomings of 2D halftoning algorithms is the loss of structural information and details during halftoning [10–15]. Generally, most digital halftoning techniques generate halftones based only on the intensity value of pixels and regardless of whether or not they are located in an area with high-frequency details of the image. Hence, sometimes they fail to represent the structures

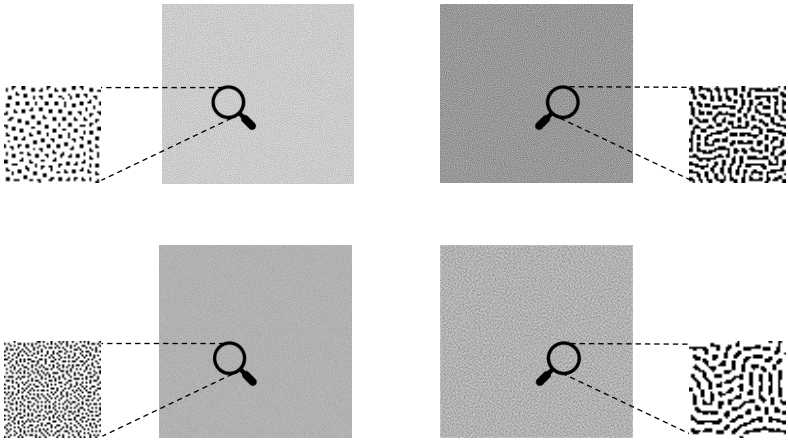

Figure 1.3 — *(Top) Different shades of gray by varying size and spacing of halftone dots. (Bottom) Different shapes of halftone dots reproduce the same gray tone. Smaller patches show an enlargement of their bigger neighbor. Note: Because the printer's characteristics were unknown to us, in the printed version of this thesis, two patches of gray at the bottom, might not appear to be of the same gray tone.*

and tones of the original image truly. In contrast to early-developed halftoning techniques, structure-aware halftoning employs the structural information of an image in addition to the pixels' intensity. The core of structure-aware halftoning methods is a halftoning algorithm coupled with mathematical models that identify and consider the original image's structural features. Many of the well-known halftoning techniques have been improved to structure-aware methods [10–15]. This thesis aims to improve the reproduction of details and structures in monochromatic and color 2D printouts and propose a structure-aware extension of an already existing halftoning algorithm (IMCDP) [16]. Details are described in Chapter 3.

Over the past few years, 3D printing has gained growing attention from industries and researchers. Full-color 3D printers, similar to 2D printers, are restricted to depositing discrete amounts of limited materials to reproduce an object's appearance. However, it is more challenging because it has more parameters contributing to the object's appearance and 3D geometry. Unlike 2D printing, which is well-researched, 3D printing and 3D surface reproduction are still evolving. However, due to major similarities between the two, many state-of-the-art 3D halftoning algorithms are developed as extensions of existing 2D algorithms [17–20]. One of the objectives of this thesis is to study the aspects of adapting and applying a high-quality 2D halftoning algorithm to halftone three-dimensional surfaces. Our primary goal is to extend the 2D algorithm to a 3D halftoning approach with minor modifications. Details are explained in Chapter 3.

1.4 Thesis Objectives

With the introduction of new printing technologies, new inks and materials, and demands for innovative applications, creating accurate reproduction of the desired visual appearance has become challenging. Therefore, there is a critical need for extensive studies to revisit the existing halftoning algorithms and develop novel approaches to produce high quality, realistic, and complex appearances that faithfully match the target appearance features. This thesis aims at developing halftoning algorithms to improve appearance reproduction in 2D and 3D printing pipelines through answering the following research questions:

- How to extend an existing 2D halftoning method to 2.5D and 3D halftoning for appearance printing with optimal dot placement?

- Can structures and patterns in images be utilized to develop improved structure-aware halftoning methods for realistic appearance printing?
- What is the effect of halftoning on reproduction of visual appearance in 3D printing?
- What are the challenges in adapting halftoning to new inks and color mixing methods in 2D print productions?

1.5 Thesis Outline

This thesis is structured as follows. Chapter 2 outlines the fundamentals of digital halftoning and reviews existing literature in digital halftoning, highlighting the significance of halftoning, different types of halftoning algorithms, and their applications. It briefly describes methods for 2D halftoning, assessment of 2D halftone images, structure-aware halftoning, and 3D halftoning. Chapter 3 summarizes the thesis's main contributions, core findings, and results. Finally, Chapter 4 provides concluding remarks and insights into the future work. Full-text publications are included as appendices in this dissertation.

CHAPTER 2

Fundamentals of Digital Halftoning

Digital halftoning is the process of converting a continuous-tone image into a binary image [6, 7]. Digital halftoning is a fundamental aspect of image reproduction in printing and imaging technologies. Many output devices, such as printers, are binary devices with a limited number of inks that can either output a colorant at a specific position or leave it blank. Halftoning techniques focus on simulating the original digital image's appearance by placing discrete dots with limited numbers of colorants.

The key idea of halftoning algorithms is based on the fact that the human visual system (HVS) functions as a low-pass filter and attenuates high frequencies [6]. Many halftoning methods reproduce the image by optimally placing dots to create a visual illusion of an image. The goal of halftoning algorithms is to minimize the difference between the original and binary images so that the error is hardly perceptible [3, 6, 7].

2.1 Halftone Structure

Halftone structure, which is the prominent attribute of halftoning algorithms, can be divided into Amplitude Modulated (AM) and Frequency Modulated

(FM) [3]. AM halftone (also known as clustered-dot halftone) produces a pattern of clustered-dot halftones with a constant frequency, where the clusters' size changes based on the gray tone [3]. The size of the clusters is proportional to the represented gray level; i.e., larger clusters correspond to darker gray tones. The FM halftone structure is made of many dispersed single dots of the same size, where the gray level is represented as a function of the frequency of the pattern, i.e., the more closely distributed black dots correspond to darker gray tones, and the more scattered distributed dots to brighter gray tones. This halftone structure is called first-order FM. Figures 2.1 (a) and (b) show examples of AM and FM halftones, respectively.

There is another type of FM, called second-order FM, in which the halftone structure forms clustered dots varying in both size and frequency. Second-order FM is also known as stochastic clustered-dot halftones. Figures 2.2 (a) and (b) show examples of second-order and first-order FM halftones, respectively. One of the advantages of the second-order FM halftoning over the first-order is that the second-order FM results in a halftone that gives a less grainy impression in the areas of an image where the tones vary smoothly (e.g., background regions in the sample image) [21].

A well-formed first-order FM halftone ensures that the quantization error, which is an inherent part of the halftoning process, is shifted into a higher frequency range that is not easily detectable by the human eye. It is shown that first-order FM halftones exhibit blue noise characteristics [22]. Blue noise is a specific distribution of noise where higher frequencies are emphasized while lower frequencies are suppressed. Unlike random or white noise, blue noise appears visually smoother, and has a more pleasant quality and it is often used to minimize visible artifacts and improve image quality. By incorporating blue noise

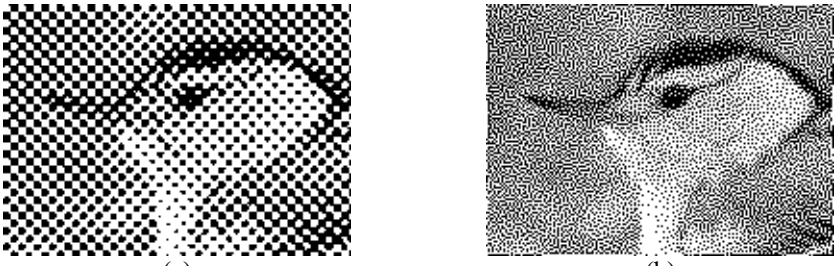

Figure 2.1 — *Examples of (a) AM (b) FM halftones.*

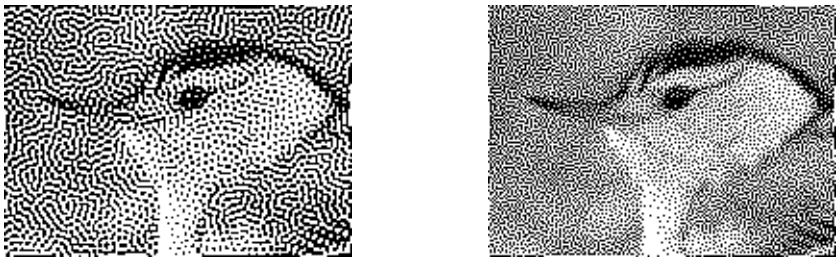

Figure 2.2 — *Examples of (a) second-order (b) first-order FM halftones.*

characteristics into the halftone pattern, the distribution of dot sizes or densities across the image will have a similar effect on higher frequencies, reducing the visibility of unwanted patterns and ensuring a smooth and continuous appearance. The blue noise principal wavelength equals the average distance between halftone dots and is calculated as in Eq. 2.1:

$$\lambda_b = \begin{cases} 1/\sqrt{g}, & 0 < g \leq 1/2 \\ 1/\sqrt{1-g}, & 1/2 < g \leq 1 \end{cases}, \tag{2.1}$$

where, g is the gray level, and λ_b is the average distance between halftone dots.

Green noise is the mid-frequency component of white noise, which, like blue noise, benefits from an aperiodic, uncorrelated structure without low-frequency graininess [23]. But unlike blue noise, green noise patterns exhibit clustering. This results in the distribution of clustered dot sizes or densities across the image, prioritizing frequencies in the middle range while suppressing both low and high frequencies. Green noise also forms aperiodic patterns that are not necessarily radially symmetric. Since the contrast sensitivity function of the human visual system is not radially symmetric, we allow green noise to have asymmetric characteristics. Like blue noise, green noise does not add a structure of its own and does not appear noisy or uncorrelated. The radially averaged power spectrum curves for different types of halftones help to study their characteristics in different frequency ranges [8]. Second-order FM halftones exhibit green noise characteristics [22]. Using green noise characteristics in halftone patterns balance smoothness and detail. By emphasizing mid-frequency components, the halftone patterns achieve a visually appealing appearance, and balance sharpness and gradual transitions. In green noise, separated neighboring

clusters are placed at an average distance of λ_g apart (center-to-center distance). The green noise principal wavelength is calculated as in Eq. 2.2:

$$\lambda_g = \begin{cases} 1/\sqrt{g/M}, & 0 < g \leq 1/2 \\ 1/\sqrt{(1-g)/M}, & 1/2 < g \leq 1 \end{cases}, \tag{2.2}$$

where, g is the gray level, and M is the cluster area. The area of a cluster is equal to the average number of pixels forming the clusters. From Eq. 2.2, one could understand that by increasing the size of the clusters, f_g (the frequency) approaches zero; and as the size of the cluster decreases to 1, which is the smallest possible cluster's size of a single pixel, f_g approaches f_b, giving the blue noise characteristics as a special case ($f_g = 1/\lambda_g$ and $f_b = 1/\lambda_b$).

However, the choice of the appropriate halftone is not always based on the frequency characteristics but also depends, among others, on the printing technology. For example, inkjet printers reproduce dispersed dots stably, but electrophotographic technology cannot create dispersed dots. Hence, first-order FM halftones work properly in inkjet printers, while in electrophotographic technology, clustered-dot (second-order FM) halftoning techniques are more suitable [9].

2.2 Halftoning Algorithms

Various halftoning approaches have been introduced over the past half a century that can be divided into three main categories:

- Threshold halftoning [6, 24]
- Error diffusion halftoning [10, 11, 25–27]
- Iterative halftoning [16, 21, 28, 29]

2.2.1 Threshold Halftoning

Thresholding algorithms are point-process techniques that convert the original image into a binary image of "1"s and "0"s based on a pixel-by-pixel comparison of pixels' intensity against a threshold value [7]. Figure 2.3 (a) and (c) illustrate continuous-tone images of a ramp of gray tones and a bird, respectively, with a dynamic range of $[0,1]$; where, a pixel with an intensity value of 0 represents a white pixel and a pixel with an intensity value of 1 represents a black pixel. As

these images are scaled between 0 and 1, the most logical threshold value would be 0.5. As expected and seen in Figures 2.3 (b) and (d), thresholding the entire image with a constant threshold value can represent only two levels of gray, either black or white. To create a halftone with impression of multiple levels of gray, it is common to use a threshold matrix rather than one fixed threshold value. Each pixel of the original image is compared with its corresponding element of the threshold matrix. If the threshold matrix is smaller than the original image, which typically is the case, the threshold matrix should be repeated in both directions to be tiled over the entire image [24].

Commonly, elements of a threshold matrix are successive positive integers starting from 1, being normalized between 0 and 1 by dividing all elements by the largest threshold value plus 1. The size of a threshold matrix greatly impacts the final appearance of the halftone image. A threshold matrix of size $n \times n$ can generate halftones with maximum $n^2 + 1$ different gray levels. Figure 2.4 illustrates examples of threshold halftoning using different threshold matrices. Figures 2.4 (a) and (d) show halftones generated using a threshold matrix of size 6×6 with elements between 1 and 18, therefore, represent 19

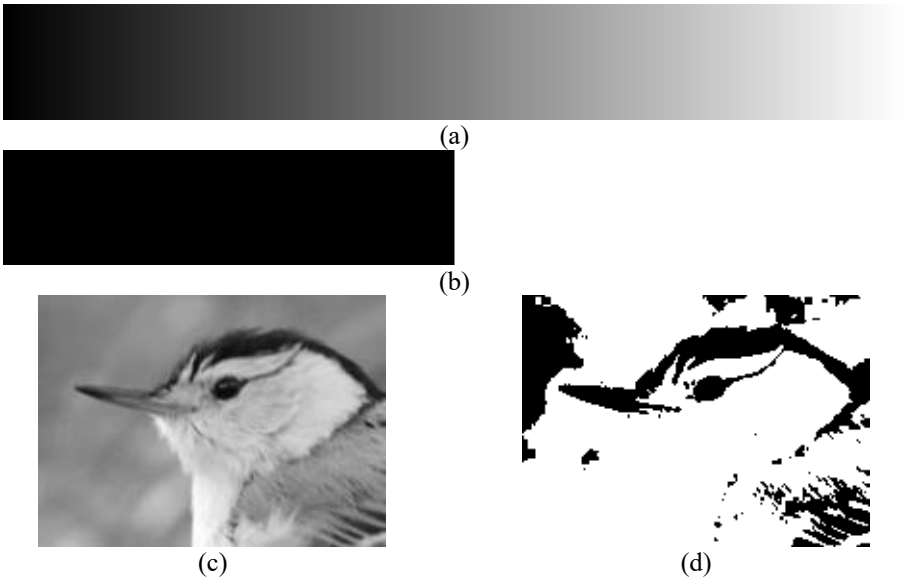

Figure 2.3 — *(a) and (c) Original continuous-tone images, where the dynamic range of pixel values is* $[0,1]$*. (b) and (d) Results after thresholding images against a threshold value of* 0.5*.*

different gray levels. Halftones in Figures 2.4 (b), (c), (e), and (f) are created using a threshold matrix of size 8×8, with elements between 1 and 32, therefore, represent 33 different gray levels.

In addition to the size, the design of a threshold matrix affects the resulting halftone. As can be seen in Figures 2.4 (b), (c), (e), and (f), even though they all used a threshold matrix of the same size, 8×8, the halftone patterns appear differently. The reason is that the successive integer elements in the threshold matrix used in Figures 2.4 (b) and (e) are placed coherently in a spiral pattern, resulting in a clustered-dot halftone pattern, while the successive integers in the threshold matrix used in Figures 2.4 (c) and (f) are set in a dispersed manner, leading to a dispersed-dot halftone pattern.

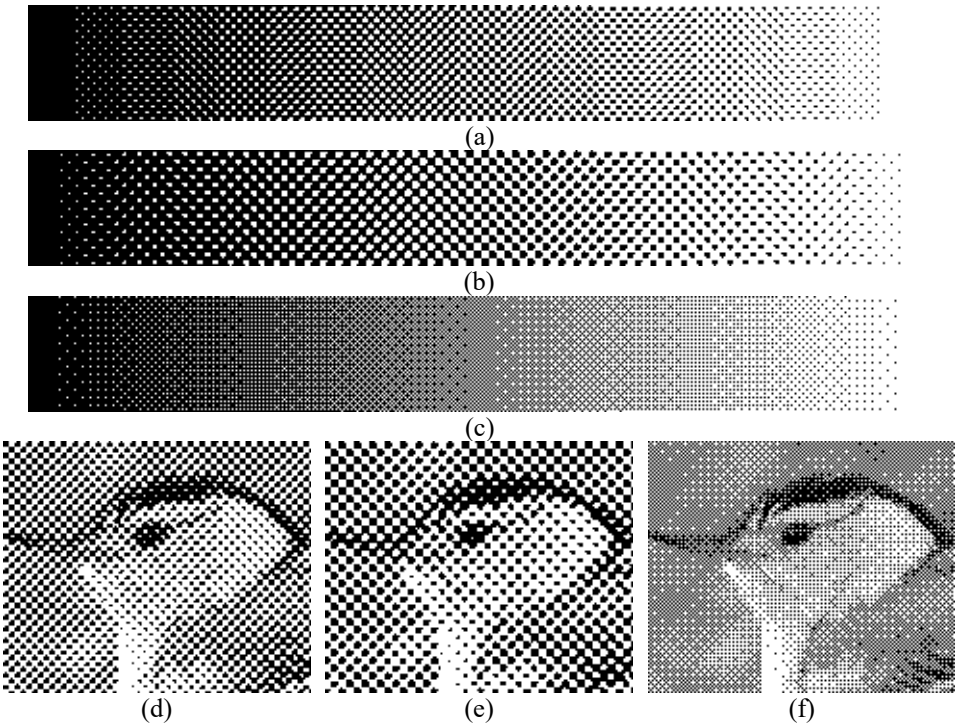

Figure 2.4 — *Examples of threshold halftoning with different threshold matrices. (a) and (d) matrix of size* 6×6*. (b) and (e) matrix of size* 8×8*, designed to form clustered dots. (c) and (f) matrix of size* 8×8*, designed to form dispersed dots.*

Threshold halftoning algorithms are simple and fast methods, but since the threshold matrices are usually smaller than the original image, they must be tiled over the entire image. As a result, halftones suffer from periodic artifacts [30, 31]. Using a larger threshold matrix can reduce such undesirable periodic patterns; however, still, outputs suffer from visible artifacts.

2.2.2 Error Diffusion Halftoning

Floyd and Steinberg first introduced error diffusion halftoning, which addressed the periodic artifacts visible in thresholding halftoning [25]. In Floyd and Steinberg's method, each pixel is compared with a fixed threshold, where the result of this comparison decides if the halftone pixel is set to 0 or 1. Then, the quantization error of each pixel (i.e., the difference between the original intensity of that pixel and the corresponding halftone value) is distributed to its neighboring pixels in a controlled manner using an error filter. Figures 2.5 (a) and (c) show the error diffusion halftone results based on Floyd-Steinberg's error filter, which, compared to Figure 2.4 minimizes the visible periodic artifacts; however, it is still affected by undesirable structural patterns. Notably, it exhibits regular patterns at multiples of the $\frac{1}{3}$ and $\frac{1}{4}$ gray levels [7, 25]. Also, at extreme gray levels of 0 and 1, it suffers from undesired regular patterns, known as worm artifacts [7, 25]. Over the years, several improved versions of Floyd and Steinberg's error filter have been proposed [26, 27]. For example, Jarvis et al. and Stucki used larger error filters to propagate the quantization error to a larger neighborhood to eliminate unwanted patterns visible in Floyd and Steinberg's method [26, 27]. Figures 2.5 (b) and (d) show examples of error diffusion using the Jarvis et al. error filter. As can be seen, the disturbing artifacts in Figure 2.5 (c) are not present in Figure 2.5 (d); however, the artifacts in the mid-tones are not eliminated.

2.2.3 Iterative Halftoning

Error diffusion algorithms reproduce halftones of higher quality compared to thresholding techniques; however, they still suffer from different artifacts, as illustrated in Figure 2.5. There is a third category of halftoning methods which can produce the highest halftone quality: iterative or search-based halftoning. In 1992, Analoui and Allebach proposed an iterative algorithm for halftoning called Direct Binary Search (DBS) [28]. The DBS algorithm starts with an arbitrary binary image (halftone image), then, the perceived error between the original image and the halftone image is computed and an iterative search for a halftone image that minimizes the error is performed. DBS has two kinds of

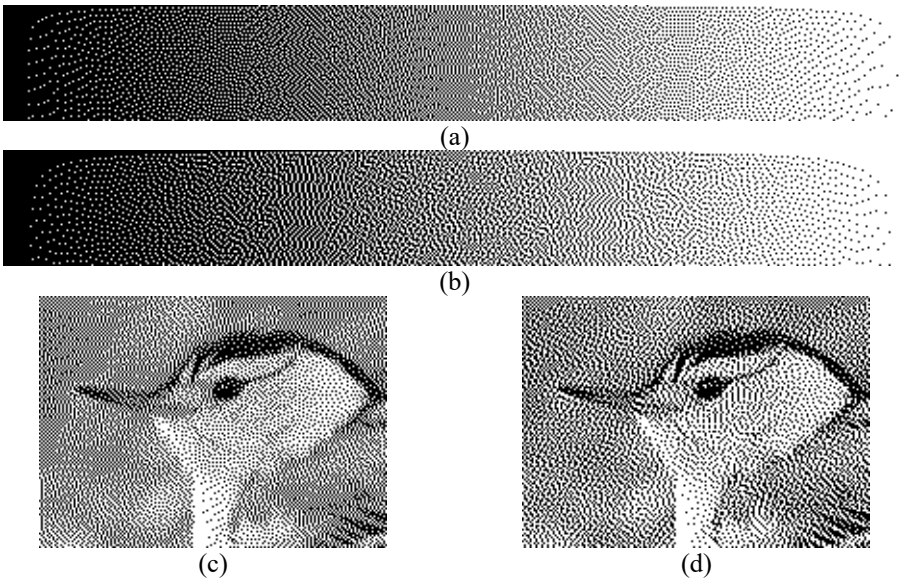

Figure 2.5 — *Examples of error diffusion halftoning algorithms using (a) and (c) Floyd and Steinberg's error filter, (b) and (d) Jarvis et al.'s error filter.*

pixel changes: toggles and swaps. Toggling means simply changing the status of the current pixel from 1 (or 0) to 0 (or 1), and swapping means swapping the value of the current pixel and one of the eight nearest pixels in its 3×3 neighborhood that has a different value. The pixels are scanned in raster order (from left to right and top to bottom). The effect of toggling/swapping its value is calculated at each pixel. If any change decreases the error, that change is accepted. The image is not changed if no toggle/swap reduces the error. One iteration is completed when every pixel in the image has been visited. The algorithm terminates when no change is accepted during an entire iteration [28]. Baqai and Allebach incorporated the printer's dot placement models with the DBS halftoning and improved tones and details reproduction in the original DBS algorithm [29]. Figures 2.6 (a) and (c) show the halftone results of implementing the DBS algorithm using the code provided in [32].

In 1998, the Iterative Method Controlling the Dot placement (IMCDP) was introduced by Gooran [16, 33, 34]. The IMCDP algorithm starts with a blank image the same size as the original image that will serve as the halftone image. The algorithm searches for the pixel holding the maximum value in the original image and places the first dot at its corresponding position in the blank halftone

image. To consider this quantization's effect, the halftone image's low-pass filtered version is subtracted from the low-pass filtered version of the original image. This process is called the feedback process, and the filter is referred to as the feedback filter, accordingly. The algorithm continues with finding the next pixel holding the highest value after the feedback process is performed. Because the average tone value in different gray-tone regions in the halftone image should be the same as the original image, the total number of black dots to be placed in each tonal region is known in advance. Hence, the IMCDP algorithm terminates when the predetermined number of black dots is placed in the halftone image [16]. The low-pass filter used in the original IMCDP algorithm is a Gaussian kernel, as shown in Eq. 2.3:

$$f(x,y) = Ke^{\frac{-(x^2+y^2)}{2\sigma^2}}, \tag{2.3}$$

where (x,y) are the spatial coordinates of pixels, K is a normalization factor to ensure that the filter elements sum to 1, and σ is the standard deviation of the Gaussian kernel. Figures 2.6 (b) and (d) show the halftone results of the IMCDP halftoning algorithm [16].

By modifying the feedback filter to Eq. 2.4, the IMCDP algorithm results in second-order FM halftones,

$$f(x,y) = K(e^{\frac{-(x^2+y^2)}{2\sigma_1^2}} - e^{\frac{-(x^2+y^2)}{2\sigma_2^2}}). \tag{2.4}$$

The filter in Eq. 2.4 is a Gaussian kernel subtracted from another Gaussian kernel with a larger standard deviation ($\sigma_1 > \sigma_2$). Parameter K is a normalization factor to ensure that the filter elements sum to 1, and (x,y) are the spatial coordinates of pixels. In second-order FM IMCDP, the single dots are first dispersed until reaching a certain tone level (decided by σ_1), and then the isolated dots start forming clusters and growing to a specific size. The maximum size of the clustered dots depends on σ_2 [21].

One important point about IMCDP is the shape of the feedback filter. In the original IMCDP, a symmetric Gaussian kernel, as defined in Eq. 2.3, is used in the feedback process. As a result, the dots are placed symmetricly in all directions. However, using a non-symmetric Gaussian kernel, as in Eq. 2.5, makes the distribution of dots non-symmetric [21],

$$f(x,y) = Ke^{-(Ax^2+2Bxy+Cy^2)}. \tag{2.5}$$

In Eq. 2.5, (x,y) are the spatial coordinates of pixels, K is a normalization factor to ensure that the filter elements sum to 1, and constants A, B, and C are calculated as:

$$A = \frac{cos^2\varphi}{2k_1\sigma^2} + \frac{sin^2\varphi}{2k_2\sigma^2}, \tag{2.6}$$

$$B = \frac{-sin2\varphi}{4k_1\sigma^2} + \frac{sin2\varphi}{4k_2\sigma^2}, \tag{2.7}$$

$$C = \frac{sin^2\varphi}{2k_1\sigma^2} + \frac{cos^2\varphi}{2k_2\sigma^2}. \tag{2.8}$$

In Eqs. 2.6 to 2.8, σ is the standard deviation of the Gaussian kernel and parameters k_1 and k_2 in the non-symmetric kernel are used to adjust the shape of the halftone structure. Setting $k_1 = k_2$ creates symmetric halftones,

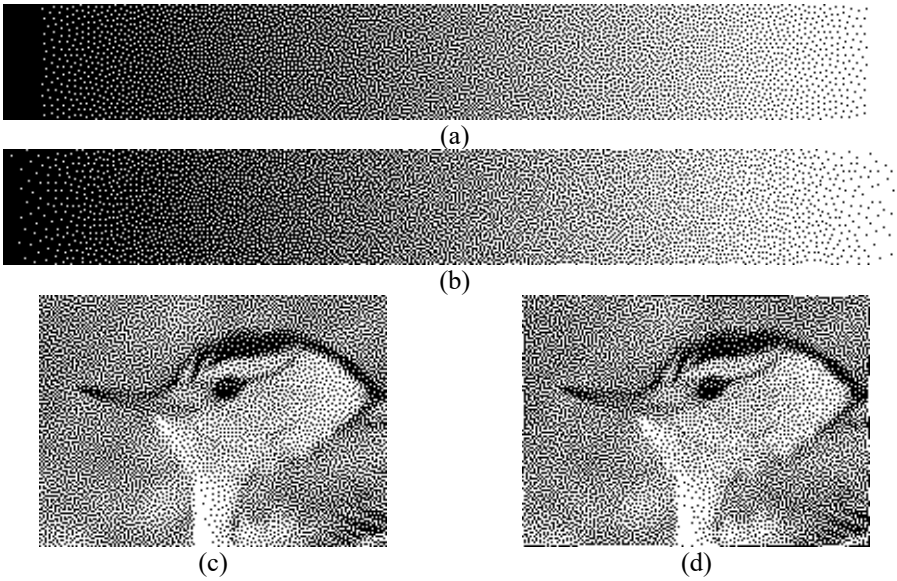

Figure 2.6 — *Examples of iterative halftoning algorithms. (a) and (c) DBS, (b) and (d) IMCDP.*

while $k_1 > k_2$ makes halftones grow faster in the vertical direction, resulting in vertical line halftones, and conversely, $k_1 < k_2$ generates halftones with horizontal alignments, resulting in horizontal line halftones. The angle φ can be used to generate line halftones in any other direction. Figure 2.7 shows a visual example of the flexibility of IMCDP in generating different halftone structures by using different Gaussian kernels in the feedback process.

It is also possible to generate non-symmetric second-order FM halftones using the following feedback filter,

$$f(x,y) = K(e^{\frac{-(x^2+y^2)}{2\sigma_1^2}} - e^{-(Ax^2+2Bxy+Cy^2)}). \tag{2.9}$$

The filter in Eq. 2.9 is a non-symmetric Gaussian kernel subtracted from a symmetric Gaussian kernel. Constants A, B, and C are calculated as shown in Eqs. 2.6, 2.7, and 2.8, where σ_1 is the standard deviation of the symmetric Gaussian kernel and σ is the standard deviation of the non-symmetric Gaussian kernel ($\sigma_1 > \sigma$).

Different halftone structures produced by the IMCDP could be combined in the same image with smooth transition [35]. The flexibility of IMCDP in generating line halftone structures makes it a robust algorithm to adaptively change the halftone structure according to the image content.

It is generally accepted that iterative halftoning algorithms achieve better quality than thresholding and error-diffusion-based algorithms, but they are often computationally expensive [16, 21, 28, 29]. A possible solution in building

Figure 2.7 — *Examples of generating non-symmetric halftones using IMCDP with (a) horizontal alignment:* $k_1 = 1, k_2 = 4$, *and* $\varphi = 0^\circ$, *(b) vertical alignment:* $k_1 = 4, k_2 = 1$, *and* $\varphi = 0^\circ$, *(c)* 30° *alignment:* $k_1 = 1, k_2 = 4$, *and* $\varphi = 30^\circ$.

threshold matrices is that the output halftone has the quality of iterative methods, which are inherently fast, similar to other threshold-based methods. For example, Gooran and Kruse introduced a method to generate image-independent threshold matrices to make the IMCDP halftoning algorithm a point-by-point method, thereby very fast [21].

2.3 Color Halftoning

Color printers use multiple colorants, typically cyan (C), magenta (M), yellow (Y), and black (K). In addition to these four primary colors, some printers, referred to as multi-channel or Hi-Fi (High-Fidelity) printers, use additional inks to reproduce more of the color spectrum. One simple yet efficient approach for color halftoning is to independently apply the monochrome halftoning algorithms to different color channels and retrieve the final color halftone image by superpositioning all the monochrome halftone images.

First, the color image, usually in RGB color space, must be separated into individual colorants (typically cyan, magenta, yellow, and black). This separation is achieved either through converting RGB to CMYK channels using the color profile of a reproduction device or by separating R, G, and B channels and converting these three to C, M, and Y colorants using mathematical formulations. Mathematical conversions do not always work accurately in a real wrold environment. For an accurate conversion from RGB to CMY, the reproduction pipleline must be accurately charaterized; thus, several methods exist to transform an RGB image to CMY color channels. For instance, in Ref. [36], Shaked et al. proposed a different approach to initialize CMYK for color error diffusion halftoning. However, a simple approach to convert the RGB to CMY colorant channels is presented in Eqs. 2.10, 2.11, and 2.12,

$$C = 1 - R, \tag{2.10}$$

$$M = 1 - G, \tag{2.11}$$

$$Y = 1 - B. \tag{2.12}$$

It is important to note that Eqs. 2.10, 2.11, and 2.12 represent a simplified way of mathematically converting the RGB to CMY colorants. In professional and commercial printing, the printer's color profile is always used to perform this conversion.

If one uses Eqs. 2.10, 2.11, and 2.12 to separate the RGB color image into C, M, and Y colorants, to consider four-color printers and generate the K colorant, it is usually assumed that full under-color removal is employed. It means that at a given position, a black dot is placed if and only if all three channels are present [3].

After separating the color channels, each of them is treated as a monochrome (grayscale) image, and the halftoning algorithm is applied to each channel separately. Once each color channel has been halftoned, the final color halftone image is created by superpositioning all color channels. Figure 2.8 illustrates a schematic of color halftoning. Because the printer's characteristics were unknown to us, the color halftone images are not adapted to the printer that prints this thesis. As a result, in the printed version of the thesis, the color halftones may not appear in accurate colors.

It is worth noting that color halftoning is not always applied independently to these RGB colors or CMYK colorant planes [37]. Many methods have been proposed to consider the effect of overlapping different colored dots to eliminate the visibility of artifacts in color halftone images [16, 37–39].

2.4 Structure-Aware Halftoning

The primary goal of halftoning methods is to preserve the local tone and structure of the original image. The early halftoning methods were developed based only on the intensity value of pixels and regardless of their position in the image, causing a loss of structural information and details. Hence, the halftone image sometimes fails to truly represent the original image's structures and tones, especially at high-frequency details. In contrast to conventional halftoning techniques, structure-aware halftoning methods employ the structural information of the original image in addition to the pixels' intensity to improve the halftone quality and better preserve both tones and structures of the original image [10, 12–14, 40, 41]. The core of structure-aware halftoning methods is a classic halftoning algorithm combined with mathematical models that identify the structural features of the original image. As a result, structure-aware halftoning algorithms generally generate halftones that better maintain structures.

Many of the well-known halftoning techniques have been improved in preserving tonal and structural details by feeding the important content of the original image as an additional input to the halftoning process. For instance, Eschbach and Knox modified the Floyd-Steinberg error diffusion by introducing threshold

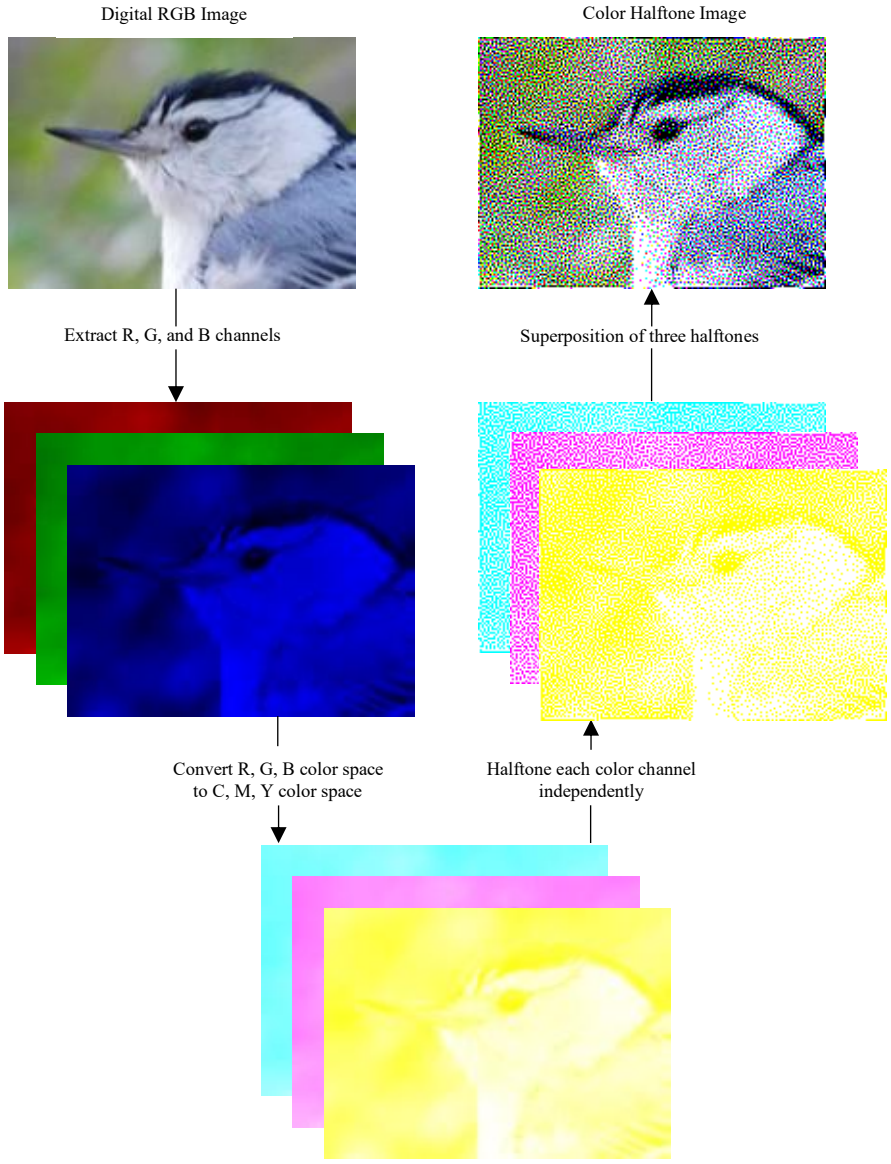

Figure 2.8 — *Color Halftoning. First, the color RGB image is separated into individual colorants (cyan, magenta, and yellow). Halftoning algorithm is applied to each channel separately. The final color halftone image is created by superpositioning all color channels.*

values derived from the image content. They used the inverse of the input image as the thresholds in the halftoning process. The amount of image content applied was controlled by multiplying a constant value in threshold adjustment. Their proposed method enhanced edge reproduction in the Floyd-Steinberg error diffusion algorithm [42].

Ostromoukhov [10] and Zhou and Fang [11] addressed the unpleasant regular artifacts, known as worm artifacts, in highlights, dark regions, and mid-tone areas and adjusted the coefficients in the error filter in a way that the undesirable regularities are mitigated. Chang et al. used the main component of local frequency in the original image as lookup table indices to modify the threshold values and the filter coefficients to improve the visual quality of halftones [40]. They built their structure-aware error diffusion method on the improvements introduced in Refs. [10] and [11].

Pang et al. proposed an optimization-based structure-aware halftoning that falls into the iterative category [12]. They defined an objective function, which measures tone fidelity (using the MSE metric) and structure similarity (using the SSIM metric) between the original and the halftone image and generated images by optimizing the objective function, i.e., maximizing the similarity [12]. Their method initiates with a random bi-tonal image containing a ratio of black and white pixels similar to the original image. In each iteration, a randomly selected pair of pixels are swapped. If the swap minimizes the error, it is accepted; otherwise, it is undone. They have shown that their proposed method preserves texture details and local tone more faithfully than Ostromoukhov's method [10].

Li and Mould employed image contrast as supplementary information and generated a contrast-aware error filter for diffusing the error to the neighborhood's pixels in Floyd-Steingberg error diffusion halftoning algorithm [13]. They also proposed implementing a dynamic scanning order to fully remove artifacts. Their method prioritized pixels based on their intensities, such that the pixels with intensity values closer to black or white are considered first, and the mid-tone regions are visited last [13].

Liu et al. proposed an entropy-based method that measures the pixel intensity's impact on the distortion of the structure and accordingly adjusts the threshold's constraints in the error diffusion halftoning algorithm [14]. Li et al. used a multi-level error diffusion technique as the core algorithm for their texture-aware halftoning [15]. They extracted texture information through edge detection and contour exclusion, then redesigned the distribution of the quantization error

such that the error is not diffused to strong textures [15].

2.5 Quality Evaluation of Halftone Images

Quality evaluation of halftone images is essential for ensuring accurate image reproduction, optimizing printing processes, and ultimately delivering high quality visual experience for users. It helps maintaining fidelity to the original image, improving print output, and enhancing user satisfaction in various applications. However, details of the structural information of the original image are often smoothed, especially at the edges, in the halftoning process. Evaluating halftone's quality ensures the maintenance of desired detail, tonal smoothness, and overall fidelity. It allows adjustments and improvements to be made during reproduction to ensure a faithful representation of the original image.

The fundamental concept of halftoning is based on the spatial integration response of the human visual system [6]. When viewing the isolated halftone dots from a sufficiently large distance, the human eyes create an illusion of the original image. The ultimate objective of halftoning algorithms is to generate a halftone image that is perceptually close to the original image and to satisfy the human observer. Thus, it is essential to understand the mechanisms of our visual perception to evaluate a halftoning algorithm.

The illusion of a continuous-tone image in the human visual system is due to a blurring effect that decreases the visual system's sensitivity in spatial resolving of fine details. This blurring effect increases with cycles per degree of visual angle. Cycles-per-degree is defined as a function of resolution and viewing distance as shown in Eq. 2.13 [43],

$$cycles/degree = \frac{R}{\frac{180}{\pi} \times \tan^{-1}(\frac{1}{D})}. \tag{2.13}$$

In Eq. 2.13, D is the viewing distance in inches, and R is the resolution in *dpi* or *ppi*. *dpi* (dots per inch) represents the number of printed dots within one inch of a printed image, and *ppi* stands for pixels per inch corresponding to the number of pixels within one inch of an image displayed on a computer display.

Eq. 2.13 suggests that at a fixed viewing distance, the higher the resolution, the higher the cycles-per-degree and, thereby, the smaller the visual angle. In other words, when the resolution increases, the sensitivity of our visual system is decreased to a larger extent, and the blurring effect in the HVS increases.

Also, the HVS has a smaller visual angle at a larger viewing distance, making it less sensitive to fine details. Therefore, the halftone dots appear more blurred to our eyes.

The contrast sensitivity function (CSF) describes the sensitivity of the HVS to different spatial frequencies in the visual stimulus. Many studies have been conducted to mathematically model the spatial integration of the HVS [6, 44–50]. Some, like Campbell et al. [50] and Mannos and Sakrison [48] modeled the CSF as a band-pass filter. However, in Refs. [44, 46, 47, 51], it was modeled as a filter with low-pass characteristics. Barten's model is more general, with adjustable parameters that can be matched to the models mentioned earlier [49]. Pappas and Neuhoff suggested that a simple Gaussian filter with a standard deviation of σ (in pixels), as calculated in Eq. 2.14, can model the CSF of the HVS efficiently [44],

$$\sigma = 0.0095\frac{\pi RD}{180}. \tag{2.14}$$

In Eq. 2.14, R defines the resolution in *dpi* or *ppi*, and D is the viewing distance in inches.

There are several types of objective image quality metrics, each designed to evaluate specific aspects of image quality, such as peak signal-to-noise ratio (PSNR), mean squared error (MSE), and structural similarity index measure (SSIM), to name a few commonly used ones [52]. However, they have yet to be particularly designed to assess the quality of halftone images and cannot be directly applied to them.

Normally, the quality of halftone reproduction is assessed by comparing the original image (viewed on a digital display) with the printed one. Therefore, to simulate different viewing conditions in evaluations of halftone images, the bluring effect of the HVS must be applied to the oringinal and halftone image before using the objective image quality metrics [12]. It means that the Gaussian-blurred original image and the Gaussian-blurred halftone image would be the inputs of the objective metrics [12]. The standard deviation of proper Gaussian filters could be calculated using Eq. 2.14, based on the corresponding viewing distance and resolution of the screen or the printer for the original and halftone image, respectively. After applying suitable Gaussian filters to the continuous-tone original image and the halftone image, the existing objective image quality metrics could be used to assess the quality of halftone

reproduction. The following subsections explain four image quality metrics widely used for assessing halftone images which we also used in this thesis.

2.5.1 Mean Squared Error

Mean Squared Error (MSE) is a mathematically-based metric that measures the average squared difference between the corresponding pixels' value of two images using Eq. 2.15 [52],

$$MSE = \frac{1}{M \times N} \sum_{i=1}^{M} \sum_{j=1}^{N} (I_x(i,j) - I_y(i,j))^2. \tag{2.15}$$

In Eq. 2.15, images I_x and I_y are of size $M \times N$. In this thesis, I_x and I_y are the Gaussian-blurred original image and the Gaussian-blurred halftone image, respectively. A lower MSE corresponds to a greater similarity between the two images.

2.5.2 Spatial CIELAB

The Commission Internationale de L'Eclairage (CIE, the International Commission on Illumination) has formulated several systems (called color spaces) that employ mathematical methods to quantify and define colors and human perception of colors. Among them, CIEXYZ and CIELAB stand out as significant color spaces.

The light-sensitive layer of the retina contains three types of receptors known as cones, which are sensitive to the three primaries, red, green and blue [3]. The CIEXYZ is a universal color space representing spectral sensitivity for a normal observer. The CIEXYZ tristimulus values (X, Y, and Z) are linked with the relative response of cones to red, green, and blue light, respectively. The CIELAB (or CIE $L^*a^*b^*$) color space represents the quantitative interplay between colors, encompassing attributes such as lightness (L) and chromaticity coordinates (a) and (b).

S-CIELAB is a spatial extension of CIELAB that can be used as a more advanced perceptual quality metric, which considers both structural and color information of an image. It evaluates image quality based on the CIELAB color space, approximating human color perception based on the resolution of the image and viewing distance [45]. It considers that small perceptual changes may impact the quality evaluation of images by human observers. In

S-CIELAB, first, the CIEXYZ representation of a color image is transformed to the opponent color space as shown in Eqs, 2.16, 2.17, and 2.18:

$$O_1 = 0.279X + 0.72Y + 0.107Z, \tag{2.16}$$

$$O_2 = -0.449X + 0.29Y - 0.077Z, \tag{2.17}$$

$$O_3 = 0.086X - 0.59Y + 0.501Z, \tag{2.18}$$

where O_1, O_2, and O_3 are the luminance, Red/Green, and Blue/Yellow opponent color components, respectively. Next, the data in each color channel is convolved by a two-dimensional separable spatial kernel of the form of a series of Gaussian functions, simulating the low-pass effect of the HVS to the corresponding color dimension, as in Eq. 2.19:

$$f = k \sum_i w_i E_i, \qquad E_i = k_i e^{-\frac{x^2+y^2}{\sigma_i^2}}. \tag{2.19}$$

The parameters k and k_i normalize the filters to sum to 1. The parameters w_i and σ_i represent the weight and standard deviation of the Gaussian kernel, respectively, and are different for each color plane. The filtered version of each color channel is then transformed back to CIEXYZ representation and after that to CIELAB. As a result, the representation of the image is called S-CIELAB, which includes both spatial filtering and CIELAB processing. Finally, the color difference between the S-CIELAB representation of two images is calculated using one of the standard CIELAB ΔE color difference formulae such as CIEDE76, CIEDE94, or CIEDE2000 [43, 45, 53]. Computation of ΔE is a pixel-by-pixel operation and, commonly, the mean of ΔE is the overall indicator of the perceived color difference between the two images. The mean value of ΔE can provide an overall idea of the perceived difference, and it is better to be accomplished by studying additional statistics such as the maximum, variance, standard deviation, median, and other percentiles of the error [43, 45].

2.5.3 Structural Similarity Index Measure

The structural similarity index measure (SSIM) is a widely used objective image quality metric that measures the structural similarity between two images (In this thesis, the Gaussian-blurred original image and the Gaussian-blurred halftone image). It considers local and global image characteristics to provide a perceptually meaningful evaluation of image quality [54]. In SSIM, extraction

of structural information is done based on human perception making it a robust and reliable method in imaging applications. SSIM aggregates three terms: luminance, contrast, and structure similarities by multiplication and yields one similarity index as shown in Eq. 2.20:

$$SSIM = [l(x,y)]^{\alpha} \times [c(x,y)]^{\beta} \times [s(x,y)]^{\gamma}. \tag{2.20}$$

In Eq. 2.20, the luminance term $l(x,y)$, the contrast term $c(x,y)$, and the structural term $s(x,y)$ are calculated using Eqs. 2.21, 2.22, and 2.23,

$$l(x,y) = \frac{2\mu_x\mu_y + c_1}{\mu_x^2 + \mu_y^2 + c_1}, \tag{2.21}$$

$$c(x,y) = \frac{2\sigma_{xy} + c_2}{\sigma_x^2 + \sigma_y^2 + c_2}, \tag{2.22}$$

$$s(x,y) = \frac{\sigma_{xy} + c_3}{\sigma_x\sigma_y + c_3}. \tag{2.23}$$

In Eqs. 2.21, 2.22, and 2.23, μ_x, μ_y, σ_x, σ_y, and σ_{xy} denote the weighted local means, standard deviations, and cross-covariance of two images x and y, respectively. Parameters c_1, c_2, and c_3 are small constants to avoid singularity. Parameters $\alpha > 0$, $\beta > 0$, and $\gamma > 0$ are used to adjust the relative importance of the three components. It is common to set $\alpha = \beta = \gamma = 1$ and $c_3 = c_2/2$ [54]. MSSIM is the mean value of SSIMs computed over blocks of size $L \times L$ pixels. The similarity between the two images is then measured by taking the average over all $L \times L$ blocks. The valid range for the MSSIM is from 0 to 1; a higher value corresponds to a higher similarity. Calculations of SSIM was based on the luminance component of images and according to Wang et al., the use of the other color components did not significantly change the performance of SSIM; however, according to them, this should not be considered generally true for color image quality assessment [54].

2.5.4 Blur Factor

MSE and MSSIM are two objective metrics widely used to assess the quality of halftone images [12–15, 55–57]. However, the sharpness/blurriness of halftone images has not been individually evaluated. Several blur metrics have been suggested in the literature to regulate and measure the occurrence of blurriness

[58–62]. In this thesis, we used the blur factor proposed by Crete et al. to assess halftone images [58]. The blur factor is based on the human perception of sharpness and is developed independent of any edge detector by only using the luminance component. The key idea of the blur factor is to blur the input image in vertical and horizontal directions. Then, the variation in the neighboring pixels is calculated as the absolute difference between the input image and its blurred version. A high variation between the input image and its blurred version corresponds to a sharp input image; conversely, a low variation shows that the input image was already blurred [58]. Crete et al. quantified the final blur metric value in the range of 0 to 1, corresponding to the sharpest and blurriest perception, respectively. The metric has also been verified through subjective tests [58].

2.6 3D Printing and 3D Halftoning

As 2D printing plays a significant role in reproducing images on flat surfaces, 3D printing expands production horizons, enabling the fabrication of intricate and complex geometries, which previously were difficult or impossible to produce. Full-color 3D printing emerged with powder-binder and layer-laminated technologies [63, 64]. However, the introduction of multi-jet (also known as poly-jet) 3D printing technologies made a revolutionary field in 3D printing where, in addition to generating merely the 3D shape, the reproduction of complex, realistic, and appealing appearance has become possible. As a result, 3D printing has exceeded its initial prototyping purpose and found applications in various industries, ranging from healthcare and automotive to architecture, cultural heritage, and fashion. It has sparked creativity and innovation in countless fields [65].

Despite their apparent differences, 2D printing and 3D printing share fundamental similarities, allowing the relatively new 3D printing field to leverage well-studied 2D printing technologies and algorithms. One of their similarities is the significance of accurate color reproduction. Over the past years, different pipelines have been proposed to reproduce the high fidelity appearance of 3D objects, focusing on generating faithful colors [17, 20, 66–71]. Most of these studies have taken advantage of the extensive knowledge and research in 2D printing to adapt 2D algorithms to the 3D domain.

The workflow of 3D printing typically consists of four main steps: voxelization, layer construction, color management, and material arrangement [66]. The input to the three-dimensional reproduction process is a 3D shape with color and

texture information. In some pipelines, additional information is incorporated to enhance the accuracy of appearance replication. For instance, Brunton et al. used translucency and color as the input signals in their proposed pipeline for fabricating spatially-varying translucency [68].

2.6.1 Voxelization

Voxelization occurs during the initial stage, where the input 3D shape is decomposed into individual voxels. A voxel is the three-dimensional equivalent of a pixel, which is a cube rather than a square. Similar to how a 2D image comprises pixels, these cubic voxels constitute the building blocks of 3D objects. An example of a voxelized sphere with a radius of 20 voxels is shown in Figure 2.9. For 3D printing purposes, commonly, a 2D image/texture is mapped onto the 3D shape and then voxelized. Figure 2.10 visualizes a grayscale image of a bird being mapped on a sephere, and then the shape is voxleized. After voxelization, the shape consists of voxles, where each voxel holds its coordinates and intensity value and it can be recognized by the printer. For a clearer visualization, an enlarged part of the voxelized shape (near the bird's wing) is shown in Figure 2.10 (d). The size of voxels in the $x-y$ plane depends on the printer's resolution in the x and y directions, and the height of voxels corresponds to the printer's resolution in the z direction, which depends on the thickness of one printed layer.

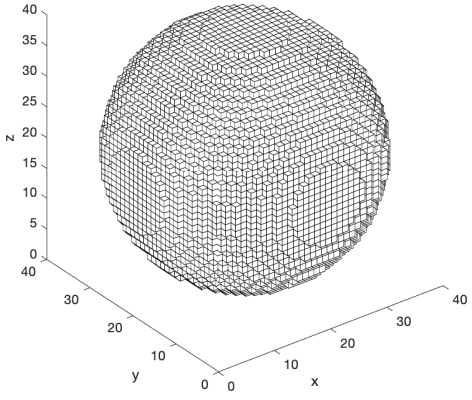

Figure 2.9 — *Voxelized sphere.*

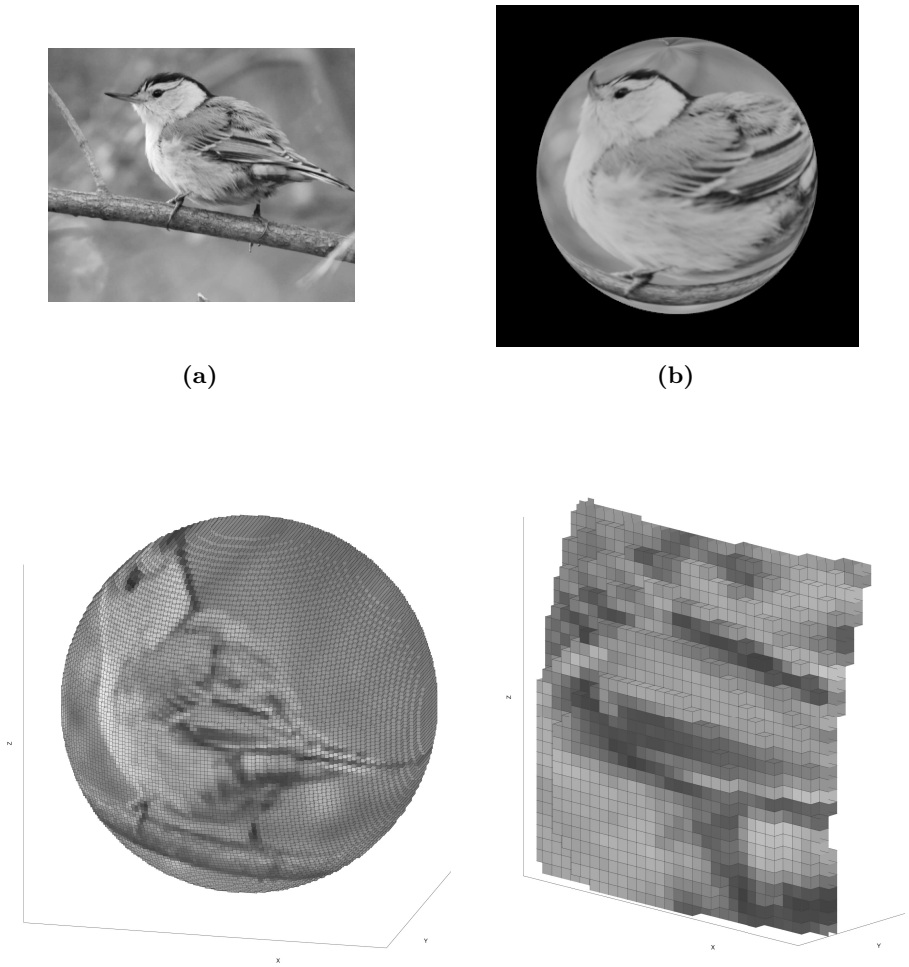

(a) **(b)**

(c) **(d)**

Figure 2.10 — *Input to a full-color 3D printing pipeline. (a) A 2D image/texture. (b) The 2D image is mapped onto a sphere. (c) The 3D shape needs to be voxelized for 3D printing purpose. (d) A zoomed-in section of the voxelized 3D object.*

2.6.2 Layer Construction

During the layer construction phase of 3D printing, the input color information, including texture (and translucency), must be transferred from the surface to the voxels within the volume of the 3D object. Merely assigning colors to the surface voxels proves insufficient in achieving the final printed objects' desired contrast and overall appearance [17, 69]. The depth of color assignment may be different for different pipelines and it needs to be charachterized according to the printer's and printing materials [17, 69].

2.6.3 Color Management

During the color management stage of the 3D printing process, a vital task involves converting the color information of the input shape into the appropriate tonal values that correspond to the available materials in the printer. This process, known as gamut mapping, fits the target colors of the input to the printer's "best" available colors and within the constraints of the printer's capabilities. Similar to 2D printers, the set of available print materials is discrete and limited, typically consisting of a small number of options (e.g., four or five different materials [17, 69]). Since each voxel can only accommodate a single material, and the number of available inks (or materials) is limited, halftoning becomes crucial in achieving full-color 3D prints.

2.6.4 Material Arrangement

Within the material arrangement phase of 3D printing pipelines, a volumetric (3D) halftoning algorithm is employed to determine the optimal placement of printing materials. As discussed earlier, 3D printing takes advantage of the available extensive knowledge and research in 2D printing in many areas, such as halftoning. Many of the proposed 3D halftoning algorithms are extensions of well-known 2D halftoning algorithms, and several studies have been conducted to adapt existing 2D halftoning methods to the 3D domain [17–20, 72–74].

Lou and Stucki were among the first who adapted 2D dithering and error diffusion to the 3D domain [72]. In Ref. [73], 3D dithering has been applied to material composition as a halftoning approach. Zhou et al. applied error diffusion to layer-based 3D object halftoning for monochrome 3D halftoning [74]. Brunton et al. developed a novel traversal algorithm based on 2D error diffusion halftoning. They adapted 2D error diffusion to 3D, producing full color with voxel-based printing technology, compatible with translucent printing materials [17]. This adaptive error diffusion halftoning approach has been

further standardized for the RGBA data format to facilitate the reproduction of both color and translucency of 3D printed objects [68]. RGB denotes red, green, and blue color components in the RGB color space, and A (Alpha) defines the translucency of the target appearance [68]. In 2017, Mao et al. proposed a novel 3D DBS halftoning algorithm that can cooperate with current 3D printing technology [18]. In 2019, Michals et al. proposed a three-dimensional extension of 2D tone-dependent fast error diffusion [19]. Their method seeks to achieve the halftone quality of iterative halftoning methods by using the concepts of DBS and error diffusion halftoning [19].

The outcome of the 3D halftoning step is a voxel-by-voxel mapping of materials (material arrangement). This mapping assigns print materials to each voxel within the volume, and it is stored on a per-slice (layer) basis. Subsequently, it is converted into a format compatible with the specific printer, tailored to its requirements and capabilities, before being sent to the device for actual printing. This process ensures that the printer receives the instructions to accurately reproduce the object with the designated materials assigned to each voxel. This strategic arrangement enables the creation of the desired color, texture, and/or translucency, ultimately resulting in the fabrication of visually pleasing and faithful representation of the target appearance. Compared to 2D printing, 3D printing still requires more development and progress. Therefore, the development of advanced 3D halftoning algorithms, which directly affect the appearance of 3D surfaces, has been a topical subject over the past few years.

CHAPTER 3

Main Contributions of the Thesis

In this section, we revisit the research questions in Chapter 1, provide a brief overview of the workflow in investigating them and summarize the main contributions in addressing them. The detailed methodology is provided in corresponding publications in the appendix of this thesis.

3.1 Extending 2D IMCDP to 3D Halftoning

The high quality halftone outputs achieved by the 2D IMCDP halftoning algorithm and its flexibility in generating different halftone structures inspired us to explore extending it to the 3D domain and improving the quality of halftone reproduction. IMCDP halftoning algorithm serves as the basis of this research, and it has been elaborated in Section 2.2.3. The first research question guided our research: How can an established 2D halftoning technique be extended to 2.5D and 3D halftoning, ensuring the optimal placement of dots for realistic appearance printing? The research aimed to address this research question led to the production of three publications *Paper A*, *Paper B*, and *Paper G*, included in the appendix of this thesis. Below, a concise summary of the conducted research is provided for clearer insights.

The primary objective regarding the 3D Iterative Method Controlling the Dot Placement (IMCDP) was to develop an approach that requires minimal adjustments for the transition from the 2D to the 3D domain. Additionally, the 3D extension of the algorithm should yield identical outcomes as its 2D counterpart in regions where the 3D shape exhibits a 2D surface behavior.

Paper A presents the main methodology to extend the 2D IMCDP algorithm to halftone 3D surfaces [75]. The proposed method could also be applied to 2.5D printing with no modification. In adapting 2D IMCDP to the 3D domain, the original algorithmic pipeline is retained, albeit with a modified method for applying the Gaussian filter. The proposed 3D halftoning method determines the optimal dot placement to produce halftone structures, resulting in halftone patterns that are fully symmetric, well-formed and free from unwanted artifacts even in extreme highlight and shadow regions. We expanded the algorithm proposed in *Paper A* to adaptively change the halftone shape and dot size based on the structures on 3D surfaces in *Paper B* [35]. It has been shown that the 3D IMCDP algorithm is a flexible method, which enables the user to control the halftone size, dot placement, and alignment according to the geometry of the surface and/or the viewing angle in combination with the structure of the texture being mapped to the surface [35].

We evaluated the performance of the developed 3D IMCDP halftoning algorithm using the voxelized sphere with the bird image, shown in Figure 2.10 (c). Figure 3.1 shows the output of the proposed 3D IMCDP halftoning algorithm. We chose a sphere for evaluation because in Ref. [19], Michals et al. compared their method to the 3D version of Floyd-Steinberg error diffusion through demonstrating the results on a sphere. Therefore, the same shape was adopted for direct method comparison. The results demonstrate that error diffusion causes more visible artifacts on specific regular longitudes and latitudes, which are removed using the 3D IMCDP algorithm. Moreover, the halftone structure generated by 3D IMCDP is more homogeneous than 3D error diffusion [75, 76].

In *Paper A* and *Paper B*, the halftoning algorithm has been applied only to the surface voxels (the outermost layer of the voxels) [35, 75]. Applying halftones only to the surface voxels results in printouts that display an undesirably low-contrast visual appearance, which is a limitation for many applications. To address this, we improved the method by incorporating a multi-layer printing approach, where the halftoning algorithm is employed within the object's volume up to specific depths. Increasing the number of layers being halftoned (the depth/thickness of color material assignment) enhances the contrast, but it concurrently induces color bleeding due to material mixing within the object

Figure 3.1 — *Output of the 3D IMCDP halftoning algorithm.*

and light scattering. Consequently, a balance must be found between the depth of applying halftones and preserving structural and color accuracy.

In *Paper G*, the 3D IMCDP method is further refined by optimizing the number of halftoned layers for each intensity level, achieving the desired contrast while mitigating unintended contamination [77]. In the proposed method, the number of halftoned layers depends on the intensity of the voxels. In light-tone regions, fewer layers are halftoned, while in dark-tone regions, the halftoning algorithm is applied deeper within the volume of the 3D object.

The output of the proposed method, in *Paper A* and *Paper B*, was evaluated by simulating the halftoning algorithm in MATLAB [35, 75]. Later, when we improved the algorithm in *Paper G*, we had the opportunity to access a commercial poly-jet 3D printer to evaluate the performance of the 3D IMCDP halftoning algorithm in a real world setup in collaboration with the Norwegian University of Science and Technology (NTNU). The results in *Paper G* were printed based on the developed 3D IMCDP, underlining that the performance of the 3D halftoning algorithm is also evaluated through practical applications on an actual 3D printer.

It is worth noting that the color measurements in *Paper G* were done by a spectrophotometer with $45^\circ : 0^\circ$ geometry. Because the printing materials are

highly translucent, commercial spectrophotometers used in 2D printing do not accurately capture the characteristics of the prints and color measurements are biased towards lower reflection [78]. A spectrophotometer with $d:8^{\circ}$ geometry is a more suitable measurement instrument for such materials. It provides more accurate color measurements for characterizing and evaluating the visual appearance of 3D prints.

3.2 Developing a Structure-Aware IMCDP

As mentioned in Section 2.4, during halftoning processes, the details of the image are often smoothed at the edges. The next research question was if structures and patterns in images can be utilized to develop improved structure-aware halftoning methods for realistic appearance printing. The primary objective involves enhancing edge reproduction beyond that achieved by the original IMCDP halftoning algorithm. The focus was on employing the content of the input image to improve the IMCDP halftoning algorithm so that the halftone structure is adaptively changed based on the image content [79, 80]. Our approach involves adjusting dot placement and aligning the halftone structure with the image's high-frequency features. As a result, the image structure's fidelity is enhanced, and the halftone pattern captures fine details and features of the original image more accurately. In addition, the degree of improvement can be controlled by the user for different parts of the image. We opt to develop the structure-aware halftoning algorithm based on the IMCDP algorithm, as it can generate line halftones with different alignments. *Paper D* and *Paper E* present our approach to addressing this research question, and they are included in the appendix of this thesis. In the following, we provide a concise summary of the conducted research to provide clearer insight.

The focus in *Paper D* was on enhancing the sharpness of grayscale halftone images while simultaneously preserving structural and tonal similarity [79]. The proposed method consists of two stages: preprocessing and halftoning. In preprocessing, the dominant orientation in the neighborhood of each pixel of the original image is identified. Subsequently, the original image is categorized into structureless (union of pixels lacking a dominant orientation in the neighborhood) and structured regions (comprising pixels with a dominant orientation in the neighborhood). Then, in the halftoning stage, different halftone structures have been used in different regions of the image based on the orientation of the dominant line.

The halftoning algorithm's novelty was in employing different Gaussian filters

during the feedback process. The filters facilitated the alignment of halftone dots along the prominent orientation within the pixels' neighborhoods. A symmetric Gaussian filter, as defined in Eq. 2.3, was employed within the vicinity of pixels located in structureless regions. On the contrary, a non-symmetric filter, as defined in Eq. 2.5, was applied within the vicinity of pixels located in structured regions. It means that the halftone structure is aligned with the dominant orientation in the pixels' neighborhoods. This approach accentuates edge information by aligning the halftone structure with the dominant orientation in the pixels' neighborhoods, consequently preserving details in the halftone image along the edges.

The proposed method was later improved in *Paper E*, where a faster technique was suggested to extract local orientation in the preprocessing step [80]. Furthermore, an adaptive approach was introduced to regulate the degree of sharpness enhancement, allowing the user to adjust the extent to which the proposed technique incorporates the structure and content across various regions within the image. The method was further extended to color halftoning. Figure 3.2 shows an example of an image being halftoned with non-structure-aware IMCDP and the proposed structure-aware alternative.

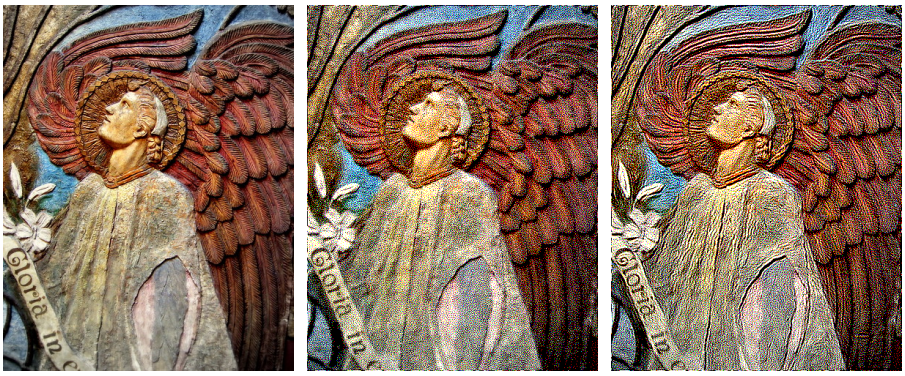

(a) **(b)** **(c)**

Figure 3.2 — *Comparing non-structure-aware IMCDP and the proposed structure-aware IMCDP halftoning technique. (a) The original image. (b) Non-structure-aware IMCDP halftone. (c) Structure-aware IMCDP halftone. Because the printer's characteristics were unknown to us, the color halftone images are not adapted to the printer that prints this thesis. As a result, in the printed version of the thesis, the color halftones in (b) and (c) may not appear in accurate colors.*

The developed structure-aware IMCDP was validated through objective and subjective image quality assessment. The results showed that the structure-aware IMCDP produces sharper halftones while retaining structural and tonal similarity. According to the results, the proposed method is more suitable for the reproduction of artworks that exhibit underlying relief structures, such as pictures of paintings featuring elevated brushstrokes, sculpted pieces, and reliefs. The structure-aware IMCDP reproduces the highly detailed appearance of these appearances, effectively conveying the tactile impression of relief structural features through a 2D reproduction to the observers. It is worth mentioning that the efficacy and applicability of the structure-aware IMCDP were further evaluated in the reproduction of pieces of artwork, described in Section 3.4.

3.3 Effect of Halftoning on Appearance of 3D Prints

The idea of this project was to apply different halftones to different regions of a 3D surface and to study the effect of halftoning on reproduction of visual appearance in 3D printing. The research addressing this question is published in *Paper C* and partly in *Paper B*. Here, a summary of the conducted research and the outcomes is presented.

The first step to study the effect of halftoning on the appearance of 3D prints is to decide how structured a region on a 3D surface is. Subsequently, we determined the appropriate halftone for individual regions with different degrees of structural complexity. In *Paper B*, we suggested dividing a 3D surface into different structural regions and applying first-order FM halftone in the more structured areas and second-order FM in flat and less structured regions; as fine details are better reproduced using first-order FM halftones. Results showed that different halftone patterns could be applied to regions of a 3D shape with different structures with a smooth transition. In *Paper B*, the types of halftones applied to different sections of the 3D shape are considered as a case study example and we did not explicitly recommend that a particular type of halftone is suitable for a given 3D surface. This requires detailed investigation and experiments that is out of scope of this thesis.

As another example, studied in *Paper C*, consider a box with sinusoidal structures with variation along one direction on the top face, as shown in Figure 3.3 (a), where an image is mapped onto it, illustrated in Figure 3.3 (b). We can apply halftones with line alignment perpendicular (Figure 3.3 (c)) or parallel (Figure 3.3 (d)) to the variation of 3D geometrical structures of the shape. As can be seen, the mapped image in Figure 3.3 (f) appears to have less 3D

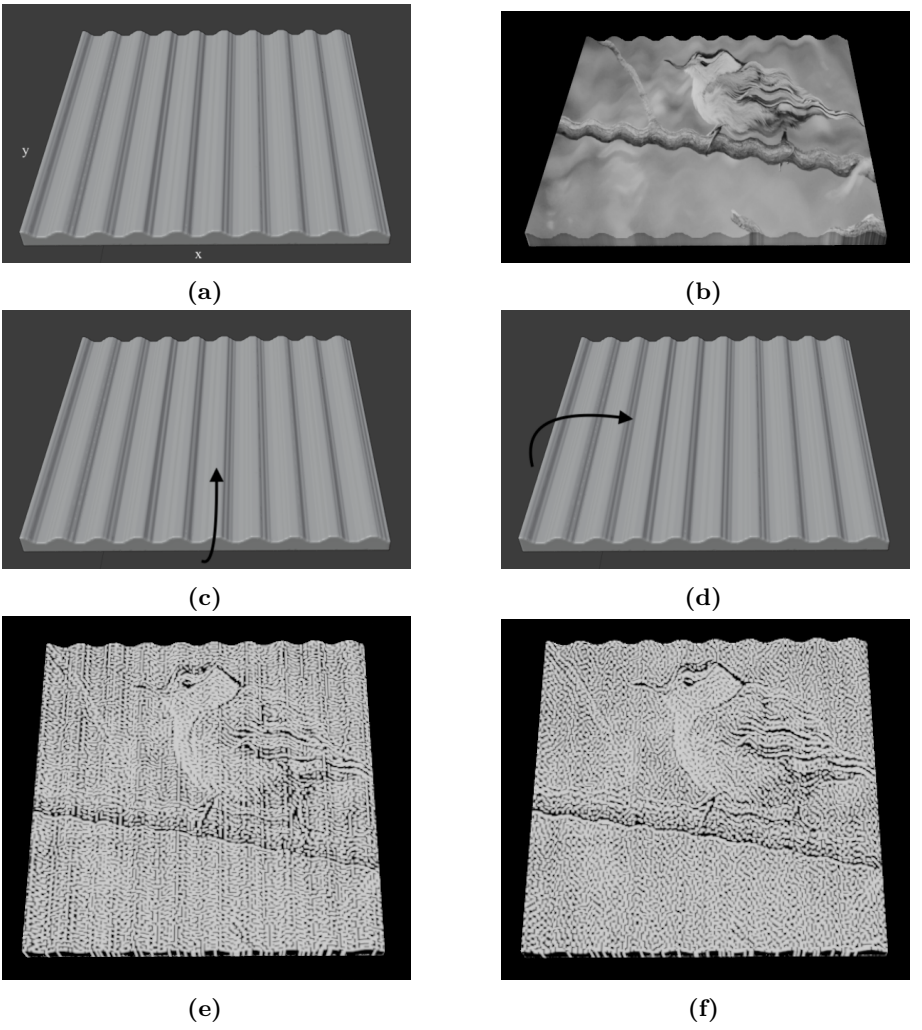

Figure 3.3 — *Effect of halftoning on the visual interpretation of the 3D shape's geometry. (a) A box with sinusoidal structures with variation along the x-axis on the top face. (b) A 2D image/texture is mapped onto the box. (c) The 3D shape will be halftoned with line structure halftones with orientation perpendicular to the variation of 3D geometrical structures of the shape. (d) The 3D shape will be halftoned with line structure halftones with orientation parallel to the variation of 3D geometrical structures of the shape. (e) Halftone output of (c). (f) Halftone output of (d).*

structure (or to be flatter) than that in Figure 3.3 (e). According to the results, applying halftones with a line structure parallel to the variation of the 3D structure could attenuate the perceived 3D geometry of the shape. However, applying line halftones perpendicular to the variation of the 3D structure could emphasize the perceived geometry of the 3D shape in the appearance of the mapped image [81].

In *Paper B* and *Paper C*, we implemented different halftone structures on different 3D shapes based on the geometric compositions of their surfaces. The findings demonstrated that one halftone variation might diminish specific 3D structures, but an alternative approach could accentuate those identical structures. It highlights the importance of tailoring 2.5D/3D dot placement to the surface elevation and intended visual outcome. Such adjustments facilitate manipulating the visual interpretation of the 3D shape's geometry and minimizing artifacts, aiming to achieve the desired appearance.

The DaVinci Color 3D printer was used to assess the impact of halftone structures on the perceived appearance and to compare the simulated halftone outputs against the experimental results. The 3D printouts agree with the simulation results in *Paper B*. Halftones possessing patterns aligned with the variations in the 3D structure of the object mitigate the perceived waviness of the 3D geometry, whereas those with perpendicular lines accentuate it.

3.4 Challenges in Adapting Halftones to New Inks in 2D Prints

This part of the research has been conducted in collaboration with the Center for Print Research, University of the West of England. The primary objective was to contribute to advancing printing techniques that are capable of replicating the color-shifting appearance inherent in natural structures. The methodology could be applied to recreate the appearance of other artistic and natural materials. Our focus was on recreating the visual essence of selected cultural heritage artifacts, primarily constructed from feather compositions, using two-dimensional printing methods.

The intricate interplay of structural coloration in feathers (like in hummingbirds and peacocks) yields iridescent effects, causing colors to change with variations in observation or illumination angles [82–84]. This phenomenon generates a sense of three-dimensional visual experience during interactions between viewers and objects, making it difficult to replicate the natural appearance of featherworks in 2D formats.

To produce angle-dependent colors, we used Spectraval™ RGB effect pigments (provided by Merck, Darmstadt, Germany). Effect pigments consist of synthetic microscopic structures (usually iridescent flakes) composed of Mica and Titanium dioxide layers. Although their large particle size (up to 25 microns) makes them unsuitable for inkjet printing, they are applicable in screen printing, flexo printing, and direct lithography [85]. For optimal color generation, the particles should lie flat on the surface, a condition best achieved through screen printing. Screen printing is a technique that involves transferring ink onto a substrate through a mesh screen. The screen is prepared with a stencil that defines the desired image or pattern. The ink is then forced through holes in the screen using a squeegee, creating a print on a substrate [86].

Effect pigments create selective light absorption and selective light scattering, resulting in a continuum of colors. It ranges from random incoherent scattering to small-scale ordered structures that produce interference colors [87]. Factors such as metal oxide thickness, size, concentration, orientation, spatial distribution of particles, and application method influence the color generated by effect pigments.

A particular halftone structure determines how dots are positioned, influencing pigments' distribution on a print. Different halftone patterns create different pigment arrangements, which subsequently change the print's visual outcome. In *Paper F*, we studied the challenges in adapting halftoning to the RGB effect pigments and color mixing methods in the 2D production of an iridescent image via screen printing.

Considering the unique properties of Spectraval™ pigments and their specific and limited range of tones (gamut) in color prints, selecting the appropriate halftoning algorithms can enhance image quality. In *Paper F*, we examined the effectiveness of different halftoning algorithms in reproducing the visual aspects of a feathered headdress using RGB pigments in screen printing [88]. The approach involved using the original IMCDP algorithm to generate first- and second-order FM halftones, along with the structure-aware version of IMCDP (introduced in *Paper E*) to create halftones which deposit pigments parallal to the high-frequency content of the target image [80].

According to the results, applying first-order FM halftones led to challenges in screen creation, potentially attributed to the dot size relative to the mesh size and exposure time. However, the second-order FM and structure-aware IMCDP approaches proved effective in achieving successful prints, mainly because the halftone dots are deposited in shape of clusters or lines, respectively.

A visual analysis confirmed that the reproductions indeed display angle dependent color variations and closely resemble the color shifts observed in the original featherworks. However, prints created using the structure-aware IMCDP displayed a more realistic appearance in replicating feathers than those made by second-order FM IMCDP. The structure-aware halftoning algorithm aligns the dot distribution (pigments) with the image content, preserving the texture and structural details of the target image. The observations showed that this algorithm accurately captures the intricate structures within the artwork's feathers and enhances the reproduction of image sharpness and detail [88].

Because special effect pigments change optical properties with different illumination and viewing angles, evaluations must be done at different angles. In the case of a visual analysis, the observer can view the print from different angles. However, a multi-angle measuring instrument should optimally be employed in addition to the visual analysis for accurate color measurement.

Printing in RGB causes a reduced color gamut and therefore posed a challenge in faithfully reproducing the full spectrum of colors in the original artwork. However, the prints employing the proposed structure-aware IMCDP method exhibited a capacity for conveying depth. The arrangement of effect pigments effectively contributed to a sense of visual depth, indicating its potential to place pigments such that they replicate the arrangement of structures responsible for the iridescent effect in real feathers.

CHAPTER 4

Concluding Remarks and Future Work

This thesis aims at developing halftoning algorithms to improve appearance reproduction in 2D and 3D printing. In this chapter, we provide concluding remarks and our insights for future work.

4.1 Concluding Remarks

Our findings contributed to answering the thesis's research questions are summarized as follows.

How to extend an existing 2D halftoning method to 2.5D and 3D halftoning for appearance printing with optimal dot placement?

An existing 2D halftoning method can be extended to 2.5D and 3D halftoning. The critical task in adapting a 2D halftoning algorithm to 2.5D or 3D domain is to ensure that at each voxel, the 3D neighborhood's working space is estimated by a 2D plane with a satisfactory degree of accuracy. In other words, the 3D surface is treated as a two-dimensional plane in every voxel's neighborhood. Then, the weights and threshold parameters of the corresponding halftoning method must be adapted to the 3D domain accordingly. Because in flat parts of the 3D shape, it mimics a 2D plane, the extended 3D halftoning technique

should perform as well as its 2D counterpart in these regions. In this research, the 2D IMCDP halftoning method has been extended to the 3D domain. The proposed method can also be applied to 2.5D printing. To reproduce the visual appearance with the desired contrast and details, the proposed method was integrated with a multi-layer printing approach, where ink is deposited at variable depths.

Can structures and patterns in images be utilized to develop improved structure-aware halftoning methods for realistic appearance printing?

Structures and patterns in images can be used to improve the halftoning techniques. Important structures of images must be extracted and fed to the halftoning algorithm as supplementary information. The feature extraction step can be performed flexibly and according to the application to improve image reproduction quality. In this research, we developed a dynamic sharpness-enhancing structure-aware halftoning method that adaptively varies the local sharpness of the halftone image based on different textures of the original image to better preserve details and structure at edges. The method is most suitable for the reproduction of artworks, such as pictures of paintings featuring elevated brushstrokes, sculpted pieces, and reliefs.

What is the effect of halftoning on reproduction of visual appearance in 3D printing?

Like in 2D, halftoning plays an integral role in reproduction of visual appearance of 3D prints. We studied the impact of applying different halftones, based on the elevation variation of 3D printed surfaces, on the reproduction of visual appearance in 3D printing. According to our findings, one type of halftone might diminish specific 3D structures, while an alternative approach could accentuate those structures. Variations in the type of halftones being applied to different parts of a 3D printed object could be used to manipulate the visual interpretation of the 3D shape's geometry in a controlled manner.

What are the challenges in adapting halftoning to new inks and color mixing methods in 2D print productions?

Halftone structures determine how dots are positioned and influence pigments' distribution on a print. However, the impact of halftoning when printing with special effect pigments is more pronounced. The interference additives (Mika), present in effect pigments, can change optical properties with illumination and viewing angle and introduce color shifts. The proposed structure-aware IMCDP makes the Mica particles in the effect pigments line up in the direction of

high-frequency details of the image, and subsequently, the print reproduces the iridescent effect of the target appearance more faithfully.

4.2 Insights into the Future Work

We showed that the proposed structure-aware 2D IMCDP halftoning technique excels in reproducing details and structures of highly detailed images. We refined the proposed 3D IMCDP halftoning algorithm to adaptively change the depth of color assignment based on the voxel's intensity. The halftone structures generated by 3D IMCDP can also be modified according to the geometry of the 3D surface. In furture work, these three approaches could be combined to develop a 3D structure-aware IMCDP, where the halftoning algorithm is aware of the 3D geometry of the printed shape as well as the color and structure of the texture being mapped onto each region of the object.

Throughout this thesis, it has been shown that the 3D IMCDP works well for grayscale halftone reproduction. There remains room to consider full-color 3D halftoning by introducing colors into the workflow of the proposed 3D IMCDP. Another prospect would be applying the 3D IMCDP halftoning algorithm to shapes with complex geometry. It requires accounting for each neighborhood's normal vector to optimize the depth of color assignment based on surface curvature and texture mapping. This optimization can decrease cross contamination and color bleeding.

Last but not least, there is a potential to enhance the visual appearance of prints made of special effect pigments through halftoning. As special effect pigments change optical properties with different illumination and viewing angles, the perceived color and shape could be controlled by changing the size and orientation of halftone dots. Using a multi-angle measuring instrument, one can accurately characterize the perceived color for different pigments' depositions at different angles. Knowing the optical properties of different halftone structures at different angles improves the reproduction of the target appearance and optimizes its aesthetic aspects for different illumination and viewing angles.

Bibliography

[1] C. Eugene, "Measurement of "total visual appearance": a cie challenge of soft metrology," *12th IMEKO TC1 & TC7 Joint Symposium on Man, Science & Measurement*, 01 2008. [pages 1, 2, and 3]

[2] J. B. Hutchings, *Food colour and appearance*. Springer Science & Business Media, 2011. [page 2]

[3] G. Sharma and R. Bala, *Digital color imaging handbook*. CRC press, 2002. [pages 2, 4, 9, 10, 21, and 26]

[4] M. R. Pointer, "Measuring visual appearance-a framework of the future. project 2.3 measurement of appearance." *National Physical Laboratory Report COAM 19*, 2003. [pages 2 and 3]

[5] D. Gigilashvili, J.-B. Thomas, J. Y. Hardeberg, and M. Pedersen, "Translucency perception: A review," *Journal of Vision*, vol. 21, no. 8, pp. 4–4, 2021. [page 3]

[6] R. Ulichney, *Digital halftoning*. MIT press, 1987. [pages 4, 9, 12, 24, and 25]

[7] D. L. Lau and G. R. Arce, *Modern digital halftoning*. CRC Press, 2018. [pages 4, 9, 12, and 15]

[8] P. Goyal, M. Gupta, C. Staelin, M. Fischer, O. Shacham, and J. Allebach, "Cost function analysis for stochastic clustered-dot halftoning based on direct binary search," in *Color Imaging XVI: Displaying, Processing, Hardcopy, and Applications*, vol. 7866. International Society for Optics and Photonics, 2011, p. 78661A. [pages 6 and 11]

[9] B. E. Cooper and D. L. Lau, "Evaluation of green noise masks for electrophotographic halftoning," in *Human Vision and Electronic Imaging*

V, vol. 3959. International Society for Optics and Photonics, 2000, pp. 613–624. [pages 6 and 12]

[10] V. Ostromoukhov, "A simple and efficient error-diffusion algorithm," in *Proceedings of the 28th annual conference on Computer graphics and interactive techniques*, 2001, pp. 567–572. [pages 6, 7, 12, 21, and 23]

[11] B. Zhou and X. Fang, "Improving mid-tone quality of variable-coefficient error diffusion using threshold modulation," in *ACM SIGGRAPH 2003 Papers*, 2003, pp. 437–444. [pages 12 and 23]

[12] W.-M. Pang, Y. Qu, T.-T. Wong, D. Cohen-Or, and P.-A. Heng, "Structure-aware halftoning," in *ACM SIGGRAPH 2008 papers*, 2008, pp. 1–8. [pages 21, 23, 25, and 28]

[13] H. Li and D. Mould, "Contrast-aware halftoning," in *Computer Graphics Forum*, vol. 29, no. 2. Wiley Online Library, 2010, pp. 273–280. [page 23]

[14] L. Liu, W. Chen, W. Zheng, and W. Geng, "Structure-aware error-diffusion approach using entropy-constrained threshold modulation," *The Visual Computer*, vol. 30, no. 10, pp. 1145–1156, 2014. [pages 21 and 23]

[15] D. Li, T. Kiyotomo, T. Horiuchi, M. Tanaka, and K. Shigeta, "Texture-aware error diffusion algorithm for multi-level digital halftoning," in *Color and Imaging Conference*, vol. 28. Society for Imaging Science and Technology, 2020, pp. 85–93. [pages 6, 7, 23, 24, and 28]

[16] S. Gooran, "Dependent color halftoning: Better quality with less ink," *Journal of Imaging Science and Technology*, vol. 48, no. 4, pp. 354–362, 2004. [pages 7, 12, 16, 17, 19, and 21]

[17] A. Brunton, C. A. Arikan, and P. Urban, "Pushing the limits of 3D color printing: error diffusion with translucent materials," *ACM Transactions on Graphics (TOG)*, vol. 35, no. 1, pp. 1–13, 2015. [pages 7, 29, and 32]

[18] R. Mao, U. Sarkar, R. Ulichney, and J. P. Allebach, "3D halftoning," *Electronic Imaging*, vol. 2017, no. 18, pp. 147–155, 2017. [page 33]

[19] A. Michals, J. Liu, A. Jumabayeva, Z. Li, and J. P. Allebach, "3D tone-dependent fast error diffusion," in *Electronic Imaging, Color Imaging XXIV: Displaying, Processing, Hardcopy, and Applications*. Society for Imaging Science and Technology, 2019. [pages 33 and 36]

[20] P. Morovič, J. Morovič, I. Tastl, M. Gottwals, and G. Dispoto, "Hans3D: a multi-material, volumetric, voxel-by-voxel content processing pipeline for color and beyond," in *Color and Imaging Conference*, vol. 25. Society for Imaging Science and Technology, 2017, pp. 219–225. [pages 7, 29, and 32]

[21] S. Gooran and B. Kruse, "High-speed first- and second-order frequency modulated halftoning," *Journal of Electronic Imaging*, vol. 24, no. 2, pp. 023 016–1–023 016–19, 2015. [pages 10, 12, 17, 19, and 20]

[22] R. A. Ulichney, "Dithering with blue noise," *Proceedings of the IEEE*, vol. 76, no. 1, pp. 56–79, 1988. [pages 10 and 11]

[23] D. L. Lau, G. R. Arce, and N. C. Gallagher, "Green-noise digital halftoning," *Proceedings of the IEEE*, vol. 86, no. 12, pp. 2424–2444, 1998. [page 11]

[24] B. E. Bayer, "An optimum method for two-level rendition of continuous tone pictures," in *IEEE International Conference on Communications, June, 1973*, vol. 26, 1973. [pages 12 and 13]

[25] R. W. Floyd, "An adaptive algorithm for spatial gray-scale," in *Proceedings of the Society of Information Display*, vol. 17, 1976, pp. 75–77. [pages 12 and 15]

[26] J. F. Jarvis, C. N. Judice, and W. H. Ninke, "A survey of techniques for the display of continuous tone pictures on bilevel displays," *Computer graphics and image processing*, vol. 5, no. 1, pp. 13–40, 1976. [page 15]

[27] P. Stucki, "Mecca-a multiple-error correction computation algorithm for bi-level image hardcopy reproduction," *IBM Thomas J. Watson Research Center, New York*, 1991. [pages 12 and 15]

[28] M. Analoui and J. P. Allebach, "Model-based halftoning using direct binary search," in *Human Vision, Visual Processing, and Digital Display III*, vol. 1666. International Society for Optics and Photonics, 1992, pp. 96–108. [pages 12, 15, 16, and 19]

[29] F. A. Baqai and J. P. Allebach, "Halftoning via direct binary search using analytical and stochastic printer models," *IEEE Transactions on Image Processing*, vol. 12, no. 1, pp. 1–15, 2003. [pages 12, 16, and 19]

[30] T. Mitsa and K. J. Parker, "Digital halftoning technique using a blue-noise mask," *Journal of the Optical Society of America A*, vol. 9, no. 11, pp. 1920–1929, 1992. [page 15]

[31] D. L. Lau, G. R. Arce, and N. C. Gallagher, "Digital halftoning by means of green-noise masks," *Journal of the Optical Society of America A*, vol. 16, no. 7, pp. 1575–1586, 1999. [page 15]

[32] S. Srin, "Efficient direct binary search, digital halftoning," https://github.com/SankarSrin/EDBS-Halftoning.git, 2019. [page 16]

[33] S. Gooran, *Hybrid and Frequency Modulated Halftoning*. Thesis LIU-TEK-LIC-1998: 61, Linköping Studies in Science and Technology, 1998. [page 16]

[34] S. Gooran, "High quality frequency modulated halftoning," Ph.D. dissertation, Linköping Studies in Science and Technology, 2001. [page 16]

[35] S. Gooran and F. Abedini, "3D surface structures and 3D halftoning," in *NIP & Digital Fabrication Conference*, vol. 2020, no. 1. Society for Imaging Science and Technology, 2020, pp. 75–80. [pages 19, 36, and 37]

[36] D. Shaked, N. Arad, A. E. Fitzhugh, and I. E. Sobel, "Color diffusion: error diffusion for color halftones," in *Color Imaging: Device-Independent Color, Color Hardcopy, and Graphic Arts IV*, vol. 3648. SPIE, 1998, pp. 459–465. [page 20]

[37] A. Agar and J. Allebach, "Model-based color halftoning using direct binary search," *IEEE Transactions on Image Processing*, vol. 14, no. 12, pp. 1945–1959, 2005. [page 21]

[38] Q. Lin and J. P. Allebach, "Color fm screen design using dbs algorithm," in *Color Imaging: Device-Independent Color, Color Hardcopy, and Graphic Arts III*, vol. 3300. SPIE, 1998, pp. 353–361.

[39] D. Lau, G. Arce, and N. Gallagher, "Digital color halftoning with generalized error diffusion and multichannel green-noise masks," *IEEE Transactions on Image Processing*, vol. 9, no. 5, pp. 923–935, 2000. [page 21]

[40] J. Chang, B. Alain, and V. Ostromoukhov, "Structure-aware error diffusion," in *ACM SIGGRAPH Asia 2009 papers*, 2009, pp. 1–8. [pages 21 and 23]

[41] N.-J. Kwak, S.-P. Ryu, and J.-H. Ahn, "Edge-enhanced error diffusion halftoning using human visual properties," in *2006 International Conference on Hybrid Information Technology*, vol. 1. IEEE, 2006, pp. 499–504. [page 21]

[42] R. Eschbach and K. T. Knox, "Error-diffusion algorithm with edge enhancement," *Journal of the Optical Society of America A*, vol. 8, no. 12, pp. 1844–1850, 1991. [page 23]

[43] G. M. Johnson and M. D. Fairchild, "A top down description of s-cielab and ciede2000," *Color Research & Application*, vol. 28, no. 6, pp. 425–435, 2003. [pages 24 and 27]

[44] T. Pappas and D. Neuhoff, "Least-squares model-based halftoning," *IEEE Transactions on Image Processing*, vol. 8, no. 8, pp. 1102–1116, 1999. [page 25]

[45] X. Zhang and B. A. Wandell, "A spatial extension of cielab for digital color-image reproduction," *Journal of the Society for Information Display*, vol. 5, no. 1, pp. 61–63, 1997. [pages 26 and 27]

[46] S. J. Daly, M. Rabbani, and C.-T. Chen, "Digital image compression and transmission system visually weighted transform coefficients," Oct. 25 1988, uS Patent 4,780,761. [page 25]

[47] R. Näsänen, "Visibility of halftone dot textures," *IEEE Transactions on Systems, Man, and Cybernetics*, vol. SMC-14, no. 6, pp. 920–924, 1984. [page 25]

[48] J. Mannos and D. Sakrison, "The effects of a visual fidelity criterion of the encoding of images," *IEEE Transactions on Information Theory*, vol. 20, no. 4, pp. 525–536, 1974. [page 25]

[49] P. G. Barten, "Physical model for the contrast sensitivity of the human eye," in *Human Vision, Visual Processing, and Digital Display III*, vol. 1666. SPIE, 1992, pp. 57–72. [page 25]

[50] F. Campbell, R. Carpenter, and J. Levinson, "Visibility of aperiodic patterns compared with that of sinusoidal gratings," *The Journal of Physiology*, vol. 204, no. 2, pp. 283–298, 1969. [page 25]

[51] S. H. Kim and J. P. Allebach, "Impact of hvs models on model-based halftoning," *IEEE Transactions on Image Processing*, vol. 11, no. 3, pp. 258–269, 2002. [page 25]

[52] M. Pedersen, J. Y. Hardeberg *et al.*, "Full-reference image quality metrics: Classification and evaluation," *Foundations and Trends® in Computer Graphics and Vision*, vol. 7, no. 1, pp. 1–80, 2012. [pages 25 and 26]

[53] M. R. Luo, G. Cui, and B. Rigg, "The development of the cie 2000 colour-difference formula: Ciede2000," *Color Research & Application*, vol. 26, no. 5, pp. 340–350, 2001. [page 27]

[54] Z. Wang, A. C. Bovik, H. R. Sheikh, and E. P. Simoncelli, "Image quality assessment: from error visibility to structural similarity," *IEEE Transactions on Image Processing*, vol. 13, no. 4, pp. 600–612, 2004. [pages 27 and 28]

[55] T. Kiyotomo, M. Tanaka, and T. Horiuchi, "Appearance-preserving error diffusion algorithm using texture information," *Electronic Imaging*, vol. 2019, no. 14, pp. 104–1, 2019. [page 28]

[56] H. Wu, T.-T. Wong, and P.-A. Heng, "Parallel structure-aware halftoning," *Multimedia Tools and Applications*, vol. 67, pp. 529–547, 2013.

[57] J. M. Guo and S. Sankarasrinivasan, "Digital halftone database (dhd): a comprehensive analysis on halftone types," in *2018 Asia-Pacific Signal and Information Processing Association Annual Summit and Conference (APSIPA ASC)*. IEEE, 2018, pp. 1091–1099. [page 28]

[58] F. Crete, T. Dolmiere, P. Ladret, and M. Nicolas, "The blur effect: perception and estimation with a new no-reference perceptual blur metric," in *Human Vision and Electronic Imaging XII*, vol. 6492. International Society for Optics and Photonics, 2007, p. 64920I. [page 29]

[59] P. Marziliano, F. Dufaux, S. Winkler, and T. Ebrahimi, "A no-reference perceptual blur metric," in *Proceedings of International Conference on Image Processing*, vol. 3. IEEE, 2002, pp. 57–60.

[60] J. Caviedes and S. Gurbuz, "No-reference sharpness metric based on local edge kurtosis," in *Proceedings of International Conference on Image Processing*, vol. 3. IEEE, 2002, pp. III–III.

[61] E. Ong, W. Lin, Z. Lu, X. Yang, S. Yao, F. Pan, L. Jiang, and F. Moschetti, "A no-reference quality metric for measuring image blur," in *Seventh International Symposium on Signal Processing and Its Applications, 2003. Proceedings.*, vol. 1. IEEE, 2003, pp. 469–472.

[62] H. Hu and G. de Haan, "Low cost robust blur estimator," *2006 International Conference on Image Processing*, pp. 617–620, 2006. [page 29]

[63] "ProJet CJP 860Pro," https://www.3dsystems.com/3d-printers/projet-cjp-860pro, 2023, accessed: March 2023. [page 29]

[64] "MCOR Technologies," https://www.treatstock.co.uk/machines/item/101-mcor-iris-hd, 2023, accessed: March 2023. [page 29]

[65] P. Urban, "Graphical 3D printing: Challenges, solutions and applications," in *London Imaging Meeting*, vol. 2020, no. 1. Society for Imaging Science and Technology, 2020, pp. 87–90. [page 29]

[66] J. Yuan, G. Chen, H. Li, H. Prautzsch, and K. Xiao, "Accurate and computational: A review of color reproduction in full-color 3D printing," *Materials & Design*, vol. 209, p. 109943, 2021. [page 29]

[67] V. Babaei, K. Vidimče, M. Foshey, A. Kaspar, P. Didyk, and W. Matusik, "Color contoning for 3D printing," *ACM Transactions on Graphics (TOG)*, vol. 36, no. 4, pp. 1–15, 2017.

[68] A. Brunton, C. A. Arikan, T. M. Tanksale, and P. Urban, "3D printing spatially varying color and translucency," *ACM Transactions on Graphics (TOG)*, vol. 37, no. 4, pp. 1–13, 2018. [pages 30 and 33]

[69] O. Elek, D. Sumin, R. Zhang, T. Weyrich, K. Myszkowski, B. Bickel, A. Wilkie, and J. Krivanek, "Scattering-aware texture reproduction for 3d printing," *ACM Transactions on Graphics*, vol. 36, no. 6, 2017. [page 32]

[70] D. Sumin, T. Rittig, V. Babaei, T. Nindel, A. Wilkie, P. Didyk, B. Bickel, J. KŖivánek, K. Myszkowski, and T. Weyrich, "Geometry-aware scattering compensation for 3D printing," *ACM Transactions on Graphics*, vol. 38, no. 4, 2019.

[71] M. M. A. Morsy, A. Brunton, and P. Urban, "Shape dithering for 3D printing," *ACM Transactions on Graphics (TOG)*, vol. 41, no. 4, pp. 1–12, 2022. [page 29]

[72] Q. Lou and P. Stucki, "Fundamentals of 3d halftoning," in *International Conference on Raster Imaging and Digital Typography*. Springer, 1998, pp. 224–239. [page 32]

[73] W. Cho, E. M. Sachs, N. M. Patrikalakis, and D. E. Troxel, "A dithering algorithm for local composition control with three-dimensional printing," *Computer-Aided Design*, vol. 35, no. 9, pp. 851–867, 2003. [page 32]

[74] C. Zhou and Y. Chen, "Three-dimensional digital halftoning for layered manufacturing based on droplets," *Transactions of the North American Manufacturing Research Institution of SME*, vol. 37, pp. 175–182, 2009. [page 32]

[75] F. Abedini, S. Gooran, and D. Nyström, "3D halftoning based on iterative method controlling dot placement," in *NIP & Digital Fabrication Conference*, vol. 2020, no. 1. Society for Imaging Science and Technology, 2020, pp. 69–74. [pages 36 and 37]

[76] S. Gooran and F. Abedini, "Three-dimensional adaptive digital halftoning," *Journal of Imaging Science and Technology*, pp. 060 403–1 – 060 403–12, 2022. [page 36]

[77] F. Abedini, R. Hlayhel, S. Gooran, D. Nyström, and A. Suneel Sole, "Multilayer halftoning for poly-jet 3D printing," in *London Imaging Meeting (Accepted, scheduled for publication in September 2023.)*. Society for Imaging Science and Technology, 2023. [page 37]

[78] C. A. Arikan, A. Brunton, T. M. Tanksale, and P. Urban, "Color-managed 3d printing with highly translucent printing materials," in *Measuring, Modeling, and Reproducing Material Appearance 2015*, vol. 9398. SPIE, 2015, pp. 251–259. [page 38]

[79] F. Abedini, S. Gooran, V. Kitanovski, and D. Nyström, "Structure-aware halftoning using the iterative method controlling the dot placement," *Journal of Imaging Science & Technology*, vol. 65, no. 6, 2021. [page 38]

[80] F. Abedini and S. Gooran, "Structure-aware color halftoning with adaptive sharpness control," *Journal of Imaging Science & Technology*, vol. 66, no. 6, 2022. [pages 38, 39, and 43]

[81] F. Abedini, S. Gooran, and D. Nyström, "The effect of halftoning on the appearance of 3D printed surfaces," in *The Advances in Printing and Media Technology: Proceedings of the 47th International Research Conference of IARIGAI*, 2021, pp. 237–243. [page 42]

[82] D. Burkhardt, "Uv vision: a bird's eye view of feathers," *Journal of Comparative Physiology A*, vol. 164, no. 6, pp. 787–796, 1989. [page 42]

[83] S. Kinoshita and S. Yoshioka, "Structural colors in nature: the role of regularity and irregularity in the structure," *ChemPhysChem*, vol. 6, no. 8, pp. 1442–1459, 2005.

[84] M. G. Meadows, M. W. Butler, N. I. Morehouse, L. A. Taylor, M. B. Toomey, K. J. McGraw, and R. L. Rutowski, "Iridescence: views from many angles," *Journal of The Royal Society Interface*, vol. 6, no. suppl_2, pp. S107–S113, 2009. [page 42]

[85] A. Trujillo-Vazquez, H. Fuller, S. Klein, and C. Parraman, "The amber project: a survey of methods and inks for the reproduction of the color of translucent objects," *Applied Sciences*, vol. 12, no. 2, p. 793, 2022. [page 43]

[86] B. Fick and B. Grabowski, *Printmaking: A Complete Guide to Materials & Process*. Laurence King Publishing, 2015. [page 43]

[87] R. Riedler, C. Pesme, J. Druzik, M. Gleeson, and E. Pearlstein, "A review of color-producing mechanisms in feathers and their influence on preventive conservation strategies," *Journal of the American Institute for Conservation*, vol. 53, no. 1, pp. 44–65, 2014. [page 43]

[88] F. Abedini, A. Trujillo-Vazquez, S. Gooran, and S. Klein, "Effect of halftones on printing iridescent colors," *Electronic Imaging*, vol. 35, pp. 1–6, 2023. [pages 43 and 44]

Appendix - Publications

The publications associated with this thesis have been removed for copyright reasons. For more details please see:

https://doi.org/10.3384/9789180752701

FACULTY OF SCIENCE AND ENGINEERING

Linköping Studies in Science and Technology, Dissertation No. 2331, 2023
Department of Science and Technology

Linköping University
SE-581 83 Linköping, Sweden

www.liu.se

LINKÖPING UNIVERSITY